UNCLASSIFIED

AD NUMBER
AD395618

CLASSIFICATION CHANGES

TO: **unclassified**

FROM: **confidential**

LIMITATION CHANGES

TO:

Approved for public release, distribution unlimited

FROM:

Distribution authorized to U.S. Gov't. agencies and their contractors; Administrative/Operational Use; JAN 1969. Other requests shall be referred to Naval Ship Systems Command, Attn: OOVIC, Washington, DC.

AUTHORITY

31 Jan 1981, Group-4, DoDD 5200.10, per document marking; USNSSC Notice 4, Apr 1979

THIS PAGE IS UNCLASSIFIED

SECURITY

MARKING

The classified or limited status of this report applies
to each page, unless otherwise marked.

Separate page printouts MUST be marked accordingly.

BOTTOM BOUNCE SONAR SIGNAL CHARACTERISTICS AND TARGET CLASSIFICATION (U)

HONEYWELL SYSTEMS & RESEARCH DIVISION

DDC
Feb 18 1990

(14) 12120-FR ✓

(11) January 1969

(6)

BOTTOM BOUNCE SONAR SIGNAL CHARACTERISTICS AND TARGET CLASSIFICATION (U) (8)

(12) 67 p.

(9)

FINAL REPORT. 12 Apr - 12 Nov 68,

(15) Contract N00024-68-C-1219 new

Naval Ship Systems Command (CODE "OOV/C")
Washington, D.C. 20360

(16) SF - 101-03-16

(17) 08733

Approved by: *Paul D. Senstad*

Paul D. Senstad
Ordnance Sciences
Research Manager

Prepared by:

(10) Richard M. Powell,
Duane H. Tack
Eugene E. Yore

```
              GROUP 4
DOWNGRADED AT 3-YEAR INTERVALS,
    DECLASSIFIED AFTER 12 YEARS
```

Honeywell Inc.
~~Systems and Research Center~~
Research Department
2345 Walnut Street
~~Roseville,~~ Minnesota 55113
St. Paul

(401799)

1472

FOREWORD

This report describes the sonar signal characteristics and classification research study performed by Honeywell Inc. , Systems and Research Center, under U. S. Naval Ship Systems Command Contract No. N00024-68-C-1219. Mr. G. Miller of the Naval Ship Systems Command provided direction for the program.

Principal authors are Dr. Duane H. Tack and Dr. Eugene E. Yore, of Honeywell's S&RC Research Department. The authors gatefully acknowledge the technical contributions and leadership of Richard M. Powell, principal investigator, and later project supervisor. Charles Johnson was program manager.

The Honeywell number assigned to this report is 12120-FR.

ABSTRACT

(C) A study of the space-time properties of active sonar echoes is made with a view toward target classification on the basis of shape and aspect at long range in the bottom bounce mode. Spectral and time cross-correlations of the echoes at two space points are examined for feasibility of signal processing with respect to requirements on the transmitted signal and transmitter-target-receiver geometries. STARLITE processing (spectral correlation) is the most promising of the two, but a detailed examination of the echo properties leads to more severe restrictions on the transmitted signal and receiver separations than previously indicated. Ideally, a wide, flat, spectral window (created by the transmitted signal), within which a band-limited spectral correlation is performed, is desired. Filtering and spreading of the signal spectrum upon reflection off an irregular, stratified, impedance bottom distorts the spectral window. This places additional constraints on the operational parameters for which the space-time properties of the echo yield target information beyond that which is available at a single receiver.

UNCLASSIFIED

CONTENTS

UNCLASSIFIED

UNCLASSIFIED

ILLUSTRATIONS

vi

UNCLASSIFIED

SECTION I
INTRODUCTION

(C) Classification clues obtainable from time-processed echoes that are useful in short-range sonar operation become somewhat less auspicious at long range in the bottom bounce mode [3]. Accurate extraction of echo length is more difficult in the low signal-to-noise ratio environment created by long propagation paths and bottom bounce losses. Target localization within the beam makes target shape and aspect information unattainable from time-processed echoes. As a result, the other clues such as positional consistency, localization within the beam, and Doppler become more significant in long-range, time-processing sonars [3]. However, space-time processing renews the possibility of extracting target shape and aspect [1, 2]. Since this information is a valuable addition to the other classification clues available at long range, this report examines the space-time properties of sound fields reflected from targets characterized as linear arrays of point reflectors with a view toward extracting target shape and aspect information for classification at long range in the bottom bounce mode.

(C) Space-time analysis of the target-reflected sound field suggests either spectral or time cross-correlations for classification signal processing. Spectral cross-correlations have been considered previously in STARLITE [2]. However, the received signals at two space points do not precisely possess the properties attributed to them in the STARLITE analysis. As a result, a reexamination of the STARLITE concept was required, leading to a special type of spectral cross-correlation and somewhat more severe constraints on its applicability. For time cross-correlations, the space-time properties of the target-reflected sound field require a compression of the time scale of one of the received signals at two space points. Time cross-correlations for target classification therefore require more complicated signal processing than spectral correlations.

1

ASSUMPTIONS

(C) The basic purpose of this study was to examine the effects of bottom reflections upon the received sound field and their ramifications to signal processing for classification. In order to limit the scope of such a task to a manageable level, extraction of target shape and aspect in the bottom bounce mode has been chosen for investigation, partly for the reasons given above and partly because it is one of the more interesting long-range classification clues from the standpoint of the space-time correlation properties of the received bottom bounce echoes. To simplify the problem and concentrate on the salient aspects of bottom bounce effects on target shape and aspect classification, stationary targets and transmitter-receivers are assumed, transmissions through water are taken to be ideal, and ambient noise and reverberation are neglected. Also, multipaths involving surface reflections are signored, and as a result, target and transmitter-receiver depths are not a factor in the analysis. Ocean depth enters only through the range of incident angles for bottom reflections since loss of signal power over the propagation path is immaterial in the assumed noiseless medium.

(U) The ocean bottom is best characterized by an irregular, stratified impedance boundary. To model these characteristics as manifested in the bottom reflection coefficient, a physical approach using the Kirchoff radiation formula is taken to model bottom reflections [7]. Because reflection and first-order scattering are linear processes, the effects of bottom reflections can ultimately be modeled by a sum of random, attenuating, delay line filters. The spectral properties of these filters depend upon the angle of incidence of the signal, the amount of irregularity in the sediment layers, and the values of the acoustic parameters (density, velocity, attenuation rate) characterizing the sediment layers.

(U) Time and scope limitations on this contract did not permit a detailed investigation of the effect of bottom reflections on target classification on

2

(U) the basis of shape and aspect. However, preliminary estimates based on the spectral properties of the bottom transfer function indicate that bottom bounce STARLITE may be practical at long range where incident angles are near grazing and the effects of surface roughness and penetration of the boundary by the sound wave minimized.

SUMMARY

(C) Section II examines the general properties of the target-reflected sound field and the resulting implications to space-time processing for classification by spectral and time cross-correlations. The analysis leads to somewhat more severe geometric and signal bandwidth constraints for spectral processing than indicated by STARLITE [2]. However, the limitations of time cross-correlations are even more severe; hence, STARLITE-like signal processing appears to be the most useful for shape and aspect classification by space-time analysis.

(U) Section III considers the effects of bottom reflections and scattering in the specular direction upon the spectral crsoss-correlations. The model for the bottom reflection coefficient is presented in Appendix A.

(U) Section IV covers conclusions and recommendations.

SECTION II
SPACE-TIME ANALYSIS

(C) This section examines the general space-time properties of the sound field reflected from a target array of point scatterers and the resulting implications to signal processing for target classification on the basis of shape and aspect. Two types of signal processing are considered: cross-correlation of the spectra of signals received at two space points, i.e., STARLITE-like processing [2], and time cross-correlations. It will be seen that the received signals do not precisely possess all the properties attributed to them in the STARLITE analysis, with the result that somewhat more severe restrictions are placed on the transmitted signal spectrum and transmitter-target-receiver geometries for successful extraction of target shape and aspect.

GENERAL SPACE-TIME PROPERTIES OF REFLECTED SOUND FIELD

(U) For the purposes of deriving the spectral properties of the target-reflected sound field, assume that an arbitrary array of $(M + 1)$ point reflectors of scattering amplitude a_i $(i = 0, 1, \ldots, M)$ is insonified by an omnidirectional transmitter through a nonrefracting, nonreflecting, dispersionless medium. In the far field, the received signal spectrum at the jth (omnidirectional) receiver is then simply

$$W_j'(\omega) = S_T(\omega) \sum_{i=0}^{M} \frac{a_i e^{-j\frac{\omega}{c_o}\left(r_T^{(i)} + r_j^{(i)}\right)}}{(4\pi)^2 r_T^{(i)} r_j^{(i)}} \tag{1}$$

where c_o is the sound velocity, $S_T(\omega)$ is the transmitted signal spectrum, $r_T^{(i)}$ is the distance from the transmitter and $r_j^{(i)}$ is the distance from the

4

receiver, respectively, to the ith point reflector in the target. At long range

$$\left. \begin{aligned} r_T^{(i)} &\simeq r_T(o) + L_i \alpha_T^{(i)} \\[2ex] r_j^{(i)} &\simeq r_h^{(o)} + L_i \alpha_j^{(i)} \end{aligned} \right\} \tag{2}$$

where L_i is the distance between the 0th and i^{th} reflectors, $L_o = 0$, $r_T^{(o)}$, and $r_j^{(o)}$ are the nominal path lengths to the target, and $\alpha_T^{(i)}$ and $\alpha_j^{(i)}$ are the direction cosines of reflector i relative to the specular directions of the transmitter and receiver, respectively, in coordinate systems having their origins at the 0th reflector. Since $r^{(o)} \gg L_i \alpha^{(i)}$ at long range, target shape and aspect information is essentially contained only in the phase of the received signals. Thus, approximating $r^{(i)}$ by $r^{(o)}$ in the amplitude but retaining Equation (2) in the phase, the spectra of the received signals at two different space points (j = 1, 2) can be written in the form

$$\left. \begin{aligned} W_1'(\omega) &= H_1(\omega) S_T(\omega) e^{-j\omega t_1} \\[2ex] W_2'(\omega) &= H_2(\omega) S_T(\omega) e^{-j\omega t_2} \end{aligned} \right\} \tag{3}$$

where

$$\left. \begin{aligned} H_1(\omega) &= \sum_{i=o}^{M} b_i e^{-j\omega \tau_i} \\[2ex] H_2(\omega) &\equiv b' \sum_{i=o}^{M} b_i e^{-j\omega \epsilon_i \tau_i} \end{aligned} \right\} \tag{4}$$

are the target transfer functions for the two viewing angles, and where

5

$$b_i = \frac{a_i}{(4\pi)^2 r_T{}^{(o)} r_1{}^{(o)}}$$

$$b' = r_1{}^{(o)}/r_2(o)$$

$$t_j = \frac{r_T{}^{(o)} + r_j{}^{(o)}}{c_o}$$

$$\tau_i = \frac{L_i}{c_o}\left(\alpha_T{}^{(i)} + \alpha_1{}^{(i)}\right)$$

$$\epsilon_i = \frac{\alpha_T{}^{(i)} + \alpha_2{}^{(i)}}{\alpha_T{}^{(i)} + \alpha_1{}^{(i)}}$$

(5)

Although Equations (3), (4), and (5) have been derived under idealized conditions, the basic functional forms of W_1' and W_2' are unchanged in a refracting, reflecting, and dispersive medium so long as refraction and dispersion are negligible over the length of the target and there are no reflecting surfaces within distances of the order of the transmitted signal duration times, c_o, from the target in the specular directions for transmission and reception. Under these conditions, refraction affects only the nominal path delays, t_j, multipath returns can be resolved in time, and dispersion and reflection alter only the shape of the transmitted signal spectrum, $S_T(\omega)$ (requiring that S_T be replaced by $S_j(\omega)$ in W_j', c.f. Section III), leaving the target functions, $H_j(\omega)$, unchanged. Thus more generally we can write

$$W_1'(\omega) = H_1(\omega)S_1(\omega)e^{-j\omega t_1} \equiv W_1(\omega)e^{-j\omega t_1}$$

$$W_2'(\omega) = H_2(\omega)S_2(\omega)e^{-j\omega t_2} \equiv W_2(\omega)e^{-j\omega t_2}$$

(6)

(C) In the case of linear arrays typical of submarine targets, $\alpha_T^{(i)} = \alpha_T$, $\alpha_j^{(i)} = \alpha_j$, and hence, $\epsilon_i = \epsilon$ for all i. Under this condition

$$H_2(\omega) = b' H_1(\epsilon\omega) \tag{7}$$

and it is recognized that $H_2(\omega)$ represents a compression ($\epsilon > 1$) or expansion ($\epsilon < 1$) of the frequency scale of $H_1(\omega)$ upon change in aspect angle. It is this property of the target transfer functions as viewed from two different space points which is exploitable in extraction of target shape and aspect. The function of signal processing for classification is then to determine whether or not Equation (7) holds, and if so, estimate ϵ to determine target aspect angles α^T and α_1, and finally, estimate τ_M to determine target length L_M. However, signal processing for classification must be accomplished with the received signal spectra, and it is evident that

$$W_2(\omega) \neq b' W_1(\epsilon\omega) \tag{8}$$

even when the path delays, t_j, are removed by appropriate shifts of the time scales of the two received signals. Basically, this results from the fact that the transmitted signal does not undergo a corresponding time scale expansion or compression by the factor, ϵ, upon reflection off an individual scatterer on the target. Thus, the inequality of (8) must be overcome by appropriate design of the transmitted signal and the signal processing methods in order that the equality of (7) can be observed, when true.

SPECTRAL CROSS-CORRELATIONS

(C) STARLITE [2] was the first space-time classification scheme to use the properties of the transfer functions of linear targets expressed in Equation (7). In particular, it was recognized in STARLITE that the inherent periodicity in the transfer function of a line target varies with aspect angle, and, over a narrow frequency band, the difference in period between the target transfer

7

(C) functions viewed at two slightly different aspect angles can be approximated by a relative shift in the frequency spectra of H_1 and H_2. As a result, the STARLITE classification scheme is to:

1) Compare the frequency spectra of two return signals to see if they are the same except for a shift in frequency. If so, the target is a line target and one can proceed to step 2.

2) Measure the frequency shift to estimate aspect angle.

3) Measure the least period of H_j to estimate target length.

All three of the above tasks can be accomplished by a cross-correlation of the frequency spectra of the two received signals.

(C) Two major constraints on the geometries for which STARLITE is applicable as listed in reference [2] are the so-called correlation condition

$$\left| \frac{\Delta f}{B_w} \right| < 0.5 \tag{9}$$

where Δf is the (cyclic) frequency shift and B_w is the bandwidth of the transmitted signals, and the resolution condition

$$\left| \tau_M \Delta f \right| > 1 \tag{10}$$

These conditions were arrived at through consideration of the properties of H_1 and H_2, but apparently ignoring the realities of inequality (8). Therefore, it is necessary to reexamine the STARLITE conditions and the special form of the spectral cross-correlation required in view of this inequality.

Spectral Correlation Function

(C) Since W_1 and W_2 do not possess the properties of H_1 and H_2 for all frequencies, it is necessary to concentrate on portions of their frequency spectra that do, i.e., narrow bands where the $S_j(\omega)$ are constant, or approximately so. As pointed out in the STARLITE analysis [2], the transmitted signal essentially provides a spectral window within which it is possible to view the target properties contained in H_1 and H_2. However, in attempting to measure these properties of the target from W_1 and W_2, the shape of the spectral window must not be permitted to obscure or influence them. To this end, we consider the spectral cross-correlation function

$$R_{12}(\Omega) = \text{Re} \int_{\omega_o - \frac{\Delta}{2}}^{\omega_o + \frac{\Delta}{2}} W_1\left(\omega - \frac{\Omega}{2}\right) W_2^*\left(\omega + \frac{\Omega}{2}\right) d\omega \qquad (11)$$

where ω_o is the (radian) carrier frequency of the transmitted signal, Ω is the relative (radian) frequency shift introduced in the two spectra, the asterisk denotes the complex conjugate, and Re indicates that the real part of the integral is taken.

(C) Ideally, the signal spectra should be constant ($S_j = A_j$) in the integration band $[\omega_o - \Delta/2, \omega_o + \Delta/2]$, for then $W_j(\omega) = H_j(\omega)$ in the integral. If the band Δ is small and the change in target aspect angle between the two receivers is small, so that $|1 - \epsilon| \ll 1$, for the integration interval we can approximate

$$\omega \tau_i = 2\pi N_i + \zeta_i + (\omega - \omega_o)\tau_i$$

$$\omega \epsilon \tau_i = 2\pi N_i + \chi_i + (\omega - \omega_o)\epsilon \tau_i \qquad (12)$$

$$\simeq 2\pi N_i + \chi_i + (\omega - \omega_o)\tau_i$$

9

(C) where N_i is an integer. Under these conditions

$$R_{12}(\Omega) = A_1 A_2 b' \Delta \sum_{i=0}^{M} \sum_{j=0}^{M} b_i b_j \frac{\sin \frac{\Delta}{2}(t_i - t_j)}{\frac{\Delta}{2}(\tau_i - \tau_j)} \cos\left[\frac{\Omega}{2}(\tau_i + \tau_j) - (\zeta_i - \chi_j)\right] \quad (13)$$

Spectral Correlation Constraints

(C) The diagonal terms, $j = i$, in Equation (13) have maxima at

$$\hat{\Omega} = \frac{(\zeta_i - \chi_i)}{\tau_i} = (1 - \epsilon) \omega_o; \ i = 1, 2, \ldots, M \quad (14)$$

by subtraction of the second line of Equation (12) from the first line and evaluating the difference at $\omega = \omega_o$. This is the desired frequency shift for line targets that we seek. They also have maxima at $\Omega \tau_i = (\zeta_i - \chi_i) \pm 2\pi m$, $m = 1, 2, \ldots$, leading to an ambiguity with which we will deal later. The off-diagonal terms do not have maxima at $\hat{\Omega}$, hence they must be rendered negligible [in order that the maximum of $R_{12}(\Omega)$ occur at $\Omega = \hat{\Omega}$] by imposing the condition

$$|\Delta \tau_{min}| \ge 12\pi, \quad \tau_{min} = \min_{i, j}(\tau_i - \tau_j) \quad (15)$$

if they are to contribute less than 10 percent of corresponding diagonal components to the value of $R_{12}(\hat{\Omega})$.

(C) Consider next the effect of nonflat signal spectra S_j on R_{12}. For illustrative simplicity, assume that the band-pass signal spectra can be approximated by $S_j(\omega) \simeq A_j \cos \beta(\omega - \omega_o)$ in the neighborhood of the carrier frequency. Then the effect of such S_j on R_{12} is to replace the sin x/x term in Equation (13) by the term

$$C_{ij} = \frac{1}{2} \cos \beta\Omega \frac{\sin \frac{\Delta}{2}(\tau_i - \tau_j)}{\frac{\Delta}{2}(\tau_i - \tau_j)} + \frac{1}{4}\left[\frac{\sin \frac{\Delta}{2}(\tau_i - \tau_j - 2\beta)}{\frac{\Delta}{2}(\tau_i - \tau_j - 2\beta)} + \frac{\sin \frac{\Delta}{2}(\tau_i - \tau_j + 2\beta)}{\frac{\Delta}{2}(\tau_i - \tau_j + 2\beta)}\right]$$

(C) For C_{ij} to be insensitive to ρ, $\Omega\beta \ll 1$ is required. If we take $\omega_0 \pm \frac{\Delta}{2}$ to coincide with the half-power points of $S_j(\omega)$, $\beta = \pi/2\Delta$ and C_{ii} differs by less than 5 percent of its value at $\Omega = 0$ if

$$\left| \frac{\Omega}{\Delta} \right| \leq 0.25 \tag{16}$$

The values of C_{ij}, $i \neq j$, are again rendered negligible by condition (15).

(C) It is necessary that $R_{12}(\Omega)$ have a single global maximum within the range of frequency shifts to be encountered if a unique $\hat{\Omega}$ is to be obtained from the correlation. A unique global maximum can be ensured by requiring that

$$\left| \Omega \tau_1 \right| \leq 2\pi \tag{17}$$

since $\tau_0 = 0 < \tau_1 < \ldots < \tau_M$, and there can then be only one $\hat{\Omega}$ for which every diagonal element in $R_{12}(\Omega)$ is maximum. Furthermore, $\hat{\Omega}$ is then readily identifiable as the first global maximum encountered either to the left or right of $\Omega = 0$. As a counter example, consider the case of just three scatterers ($M = 2$) and $\tau_2 = 3\tau_1/2$. If condition (17) were violated and the desired global maximum occurred at $\hat{\Omega}\tau_1 = 2\pi + \gamma$, $0 < \gamma \leq 2\pi$, there is also a global maximum at $\tilde{\Omega}\tau_1 = \gamma - 2\pi = \zeta_1 - \chi_1 - 4\pi$, since then $\tilde{\Omega}\tau_2 = \zeta_2 - \chi_2 - 6\pi$. Since $\tilde{\Omega}$ is closer to the origin than $\hat{\Omega}$, it would be mistaken for the desired frequency shift and an erroneous estimate of $_e$, and hence target aspect and length, would be made. Although this example is based upon commensurate target highlight delays τ_1, in practice they would probably only have to be approximately commensurate to generate this kind of error if the ambiguity condition (17) is not met, since the maxima of the fluctuating components in $R_{12}(\Omega)$ are quite broad. Note that conditions (17) and (15) yield a somewhat stronger constraint than (16), since together they imply $12\pi/\Delta \leq \left| \Omega \tau_{min} \right| \leq \left| \Omega \tau_1 \right| \leq 2\pi$, or $\left| \Omega/\Delta \right| \leq 1/6$. Thus, (15) is a stronger condition for correlation than (16).

(C)   Limitations on the minimum measurable frequency shift in $R_{12}(\Omega)$ are more a function of the ability to determine that a global maximum of R_{12} has been achieved in the presence of noise than to measure the period of the most rapidly fluctuating component in $H_j(\omega)$ as implied by the STARLITE resolution condition (10).   At signal-to-noise ratios sufficient for detection, it is reasonable to expect that one would be able to ascertain the difference between a zero and a maximum in each significant correlation component in R_{12}.   Since the term with the smallest delay requires the largest variation in Ω between a zero and an adjacent maximum, the resolution condition for determination of a global maximum of R_{12} in the presence of noise is approximately

$$|\Omega \tau_1| \geq \frac{\pi}{2} \tag{18}$$

(C)   In summary, the significant constraints on spectral processing for classification of arrays of point scatterers are:

1)   Correlation condition

$$|\Delta \tau_{min}| \geq 12\pi$$

2)   Ambiguity condition

$$|\Omega \tau_1| \leq 2\pi$$

3)   Resolution condition

$$|\Omega \tau_1| \geq \frac{\pi}{2}$$

Additional STARLITE conditions [2] are the Fresnel condition, which is not constraining at long range, and the thickness condition which limits the apparent length-to-diameter, D_s, of submarine targets by the condition [2]

$$\left| \frac{L_M \sin \phi}{D_s} \right| > 4$$

12

(C) where ϕ is the target aspect angle (see Figure 1). These constraints can be untenable if significant scatterers in the target are too close together. For example, the correlation condition is violated for target highlight delays separated by less than 10 msec at a signal bandwidth, B_w, of 600 Hz. It would seem, therefore, that successful classification of targets that behave acoustically as arrays of point scatterers by spectral processing cannot depend on extraction of all target highlight delays, but rather must rely on extraction of only those widely spaced highlights such as the bow, conning tower, and stern of a submarine.

Example

(C) To examine briefly the implications of the constraints of conditions (15), (17), and (18) on reciever separations and the transmitted signal spectrum, consider the simple two-dimensional STARLITE geometry of Figure 1 where the transmitter and one receiver are positioned side by side. For this geometry, the aspect angle, ϕ, is defined to lie in the range of $0° \leq \phi \leq 180°$, with beam aspect at $0°$ or $180°$ and bow or stern aspect at $90°$. Also, the following approximations

$$\epsilon = \frac{1}{2} [1 + \cos \Psi - \cot \phi \sin \Psi] \simeq 1 - \frac{\Psi}{2} \cot \phi$$

$$D \simeq \frac{r_T^{(o)} \Psi}{\sin \theta} \tag{19}$$

hold at long range $(D/r_T^{(o)} << 1, \; r_T^{(o)} = r_1(o) \simeq r_2^{(o)}, \; \Psi << 1)$. Assuming a target length of 90 m and just three significant scattering surfaces, $\tau_L = \tau_2$ $(\phi = \pi/2) = 120$ msec for $c_o = 1.5$ Km/sec. It is also reasonable to assume that $\tau_{2/3} \leq \tau_1 \leq 2\tau_{2/3}$ for the target delays associated with the conning tower. Signal bandwidth requirements can be fixed using the STARLITE thickness constraint [2] which limits the minimum aspect angle for classification to

13
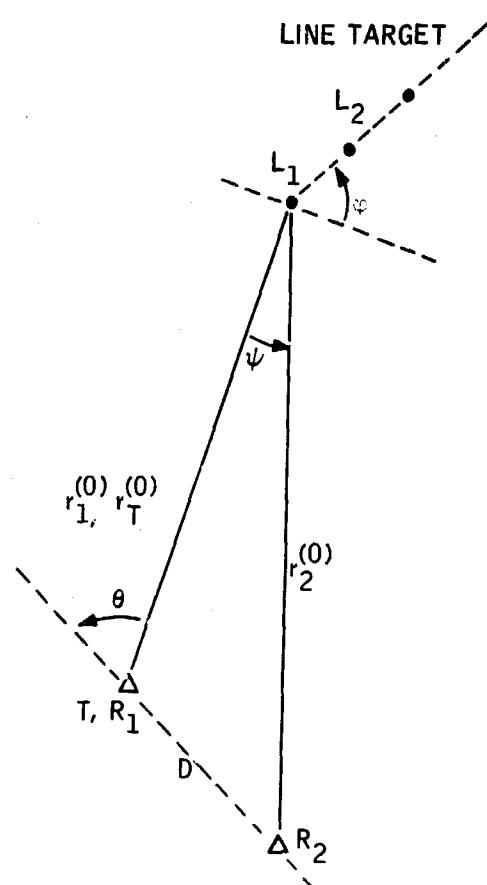
Figure 1. STARLITE Geometry

14

(C) $\phi \simeq 15°$ in this case. Then, since $\tau_{2/3} \leq \tau_{min} \leq \tau_{2/2}$, constraint (15) is satisfied for bandwidths $B_w \equiv \Delta/2\pi$, i.e.,

$$400 \text{ Hz} \leq B_w \leq 600 \text{ Hz} \tag{20}$$

Assuming that signal bandwidths of one-tenth the carrier frequency can be readily generated, let $f_o = \omega_o/2\pi = 6$ KHz. Maximum receiver separations, D, are required when τ_1 is a minimum. Thus, for $\tau_1 = \tau_{2/3}$, constraints (17) and (18) evaluated at $\hat{\Omega} = (1 - \varepsilon)\omega_o$ yield

$$2.08 \times 10^{-3} \leq \Psi \left| \cos \phi \right| \leq 8.33 \times 10^{-3} \tag{21}$$

under these conditions. Acceptable receiver separations at ranges $r = r_T^{(o)}$ of 20K and 40K yards and at $\theta = 90°$ implied by (21) are plotted in Figure 2 as a function of aspect angle, ϕ. Corresponding STARLITE constraints [2], c.f. Equations (9) and (10), are about 4/3 larger on the minimum separation, and for all practical purposes, unbounded above for the conditions of this example. A receiver separation of about 175 yards would permit extraction of target shape and aspect for $15° \leq \phi \leq 60°$ and $120° \leq \phi \leq 165°$ at $\theta = 90°$ and $20K \leq r \leq 40K$ yards. Although this is probably an acceptable receiver separation distance, the constraints are tight and do not permit much flexibility in range and bearing for fixed D. In addition, the signal bandwidth requirements are an order of magnitude larger than the bandwidths used in the initial STARLITE trials [2]. It therefore appears that some flexibility in choosing receiver separations as function of range and bearing is necessary for target shape and aspect classification by spectral cross-correlation.

TIME CROSS-CORRELATIONS

(U) After compensation for the path delays, t_j, the functional form of the received signals in the time domain is

15
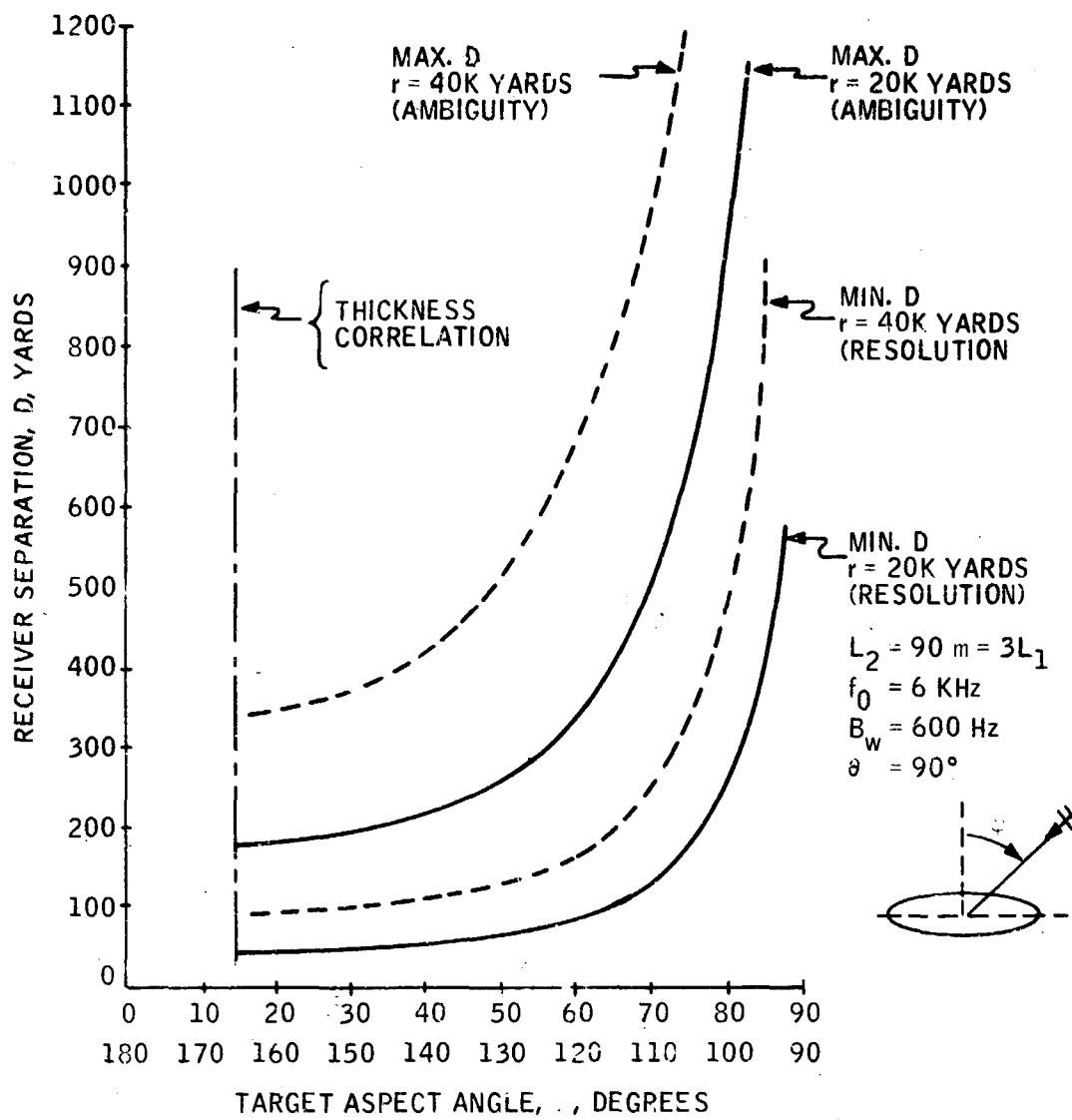
(C) Figure 2. Receiver Separation Constraints versus
Target Aspect Angle for the Example (U)

16

$$w_1(t) = \sum_{i=o}^{M} b_i s_1(t - \tau_1) \tag{22}$$

$$w_2(t) = b' \sum_{i=o}^{M} b_i s_2(t - \epsilon_i \tau_i) \tag{22}$$

In order that w_1 and w_2 achieve maximum correlation when $\epsilon_i = \epsilon$ a compression ($\epsilon > 1$) or expansion ($\epsilon < 1$) of the time scale by the amount ϵ must be performed in order that the signal component reflected off the ith scatterer in w_2 have the same delay as the corresponding component in w_1 for every i. Thus, we seek the time scaling ϵ of w_2 such that

$$\hat{w}_2(t) = b' \sum_{i=o}^{M} b_1 s_2[\epsilon (t - \tau_i)] \tag{23}$$

Suppose that an estimate of ϵ is $\tilde{\epsilon}$, yielding

$$\tilde{w}_2(t) = b' \sum_{i=o}^{M} b_1 s_2[\tilde{\epsilon} (t - \upsilon \tau_i)] \tag{24}$$

where $\upsilon = \epsilon / \tilde{\epsilon}$, and consider the time cross-correlation of w_1 and $\tilde{w}_2$

$$R_{12}(\tau) = \int_{-\infty}^{\infty} w_1(t) \tilde{w}_2(t - \tau) dt = \frac{1}{2\pi} \int_{-\infty}^{\infty} W_1(\omega) \tilde{W}_2^*(\omega) e^{j\omega\tau} d\omega \tag{25}$$

Since

$$\tilde{W}_2(\omega) = \frac{b'}{\tilde{\epsilon}} S_2\left(\frac{\omega}{\tilde{\epsilon}}\right) \sum_{i=o}^{M} b_i e^{-j\omega\upsilon\tau_i} \tag{26}$$

$R_{12}(\tau)$ can be written in the form

$$R_{12}(\tau) = b' \sum_{i=o}^{M} b_1^2 R_{s_1 s_2}[\tau - (1 - \upsilon) \tau_i]$$

$$+ b' \sum_{i=1}^{M} \sum_{j=o}^{i=1} b_i b_j \left\{ R_{s_1 s_2}[\tau - (\tau_1 - \upsilon \tau_j)] + R_{s_1 s_2}[\tau + (\upsilon \tau_i - \tau_j)] \right\} \tag{27}$$

where

$$R_{s_1 s_2}(\tau) = \frac{1}{2\pi\tilde{\epsilon}} \int_{-\infty}^{\infty} S_1(\omega) S_2^* \left(\frac{\omega}{\tilde{\epsilon}}\right) e^{j\omega\tau} d\omega \qquad (28)$$

(U) The functional form of $R_{12}(\tau)$, Equation (27), is sufficient to give us some clues as to the utility of the time cross-correlation in space-time classification on the basis of target shape and aspect. Although the carrier frequency has not been explicitly removed in the preceding analysis, we are interested in the correlation of the envelopes of w_1 and $\tilde{w}_2$, or alternatively, the envelope of $R_{12}(\tau)$.

(U) At $\tilde{\epsilon} = \epsilon$, $\upsilon = 1$ and the classification condition is achieved by maximizing the diagonal elements in $R_{12}(\tau)$ at $\tau = 0$. However, the off-diagonal elements do not have maxima at $\tau = 0$. Hence, they must be rendered negligible by a signal bandwidth constraint similar to that of Equation (14).

Resolution Condition

(C) Resolution of the diagonal components in $R_{12}(\tau)$ places even more severe restrictions on its properties. If we require a variation of the slowest varying component in the envelope of $R_{12}(\tau)$ of the same order of magnitude as that which was required for the slowest varying component in $R_{12}(\cap)$, then we require that $R_{s_1 s_2} [(1 - \epsilon) \tau_1]$ be small compared with $R_{s_1 s_2}(0)$, or approximately

$$| 1 - \epsilon | \tau_1 B_w \stackrel{\sim}{>} 1 \qquad (29)$$

Comparison of this resolution condition with that of (18) for spectral correlations at $\Omega = \hat{\Omega} = (1 - \epsilon)\omega_0$ shows that spectral processing holds a distinct advantage over time processing in that the carrier frequency, f_0, rather than the signal bandwidth, B_w, appears on the left in the resolution condition for spectral processing. Since $| 1 - \epsilon |$ is directly proportional to the receiver

(C) separation and $f_o > B_w$, the resolution condition for spectral correlations will be met with shorter receiver separations than those required for time correlations. As an example, for the same conditions as the example discussed in connection with spectral cross-correlations, condition (29) reduces to

$$|\Psi \cos \phi| \overset{\sim}{>} 0.08 \tag{30}$$

which, by comparison with condition (21), indicates that more than an order of magnitude larger receiver separations, D, would be required for time correlations than for spectral correlations. The receiver separation could be reduced by increased signal bandwidths, but it is doubtful that an order of magnitude reduction could be achieved and still keep the carrier frequency in the low-to-mid-kilocycle range required for long-range propagation.

Linear FM Signals

(U) Before concluding the discussion of time correlation, the important special case of linear FM (LFM) signals should be examined, since it turns out that the time cross-correlations of the envelopes of compressed LFM pulses have the resolution properties associated here with time processing, whereas direct time cross-correlations of the envelopes of the received LFM echoes have the properties of spectral correlations.

(C) Consider received LFM pulse components s_j in w_j of the form

$$s_j(t) = A_j e^{j(\omega_0 t + \frac{1}{2} \mu t^2)} [u(t + T_0) - u(t - T_0)] \tag{31}$$

where u(t) is the unit step function. For correlation after pulse compression we assume that the received signals are processed by a matched filter having the transfer function

$$H_f(\omega) = \exp \left[\frac{j(\omega - \omega_0)^2}{2\mu} \right] \tag{32}$$

19

(C) with the result that the compressed signal pulse is [22]

$$s_j'(t) = A_j \sqrt{\frac{2\mu T_0^2}{\pi}} \; \frac{\sin \lambda T_0 t}{\mu T_0 t} \; e^{j(\omega_0 t - \frac{1}{2}\mu t^2 + \frac{\pi}{4})} \tag{33}$$

From Equation (28), the time correlation of the envelopes of s_1' and s_2' (at $\tilde{\epsilon} = 1$) is then

$$R_{s_1' s_2'}(\tau) = A_1 A_2 \frac{T_0}{2\pi^2} \frac{\sin \mu T_0 \tau}{\mu T_0 \tau} \tag{34}$$

But $B_w = \mu T_0/\pi$ for the LFM pulse; hence, for $R_{s_1' s_2'}$ to have its first correlation zero at $\tau = \pi/\mu T_0 \leq |1 - \epsilon|\tau_1$, condition (29) is required. We note, therefore, that reduction of the reverberation noise level in STARLITE processing by LFM pulse compression as suggested by Wiekhorst [23] is obtained only at the expense of increased receiver separation requirements.

(C) It is well known that the envelope of an LFM pulse is a good approximation to its spectrum; hence, a time cross-correlation of the envelopes of uncompressed LFM echoes should be a good approximation to their spectral cross-correlation. To investigate this case mathematically, consider that within the time interval $[T_0 + \tau_m, \; T_0 - \tau_m]$, or $[-T_0 + \epsilon\tau_m, \; T_0 - \epsilon\tau_m]$, whichever is the smaller, the received signals can be written in the form

$$w_1(t) = \sum_{i=0}^{M} b_i s_1(t - \tau_i) = s_1(t) \sum_{i=0}^{M} b_1 e^{-j[(\omega_0 + \mu t)\tau_i - \frac{1}{2}\mu\tau_i^2]}$$
$$= A_1^{-1} s_1(t) Z_1(t) \tag{35}$$

$$w_2(t) = b' \sum_{i=0}^{M} b_i s_2(t - \epsilon\tau_i) = s_2(t) b' \sum_{i=0}^{M} b_i e^{-j[(\omega_0 + \mu t)\epsilon\tau_i - \frac{1}{2}\mu\epsilon^2\tau_i^2]}$$
$$= A_2^{-1} s_2(t) Z_2(t)$$

when s_j is given by Equation (31), and z_j is therefore the envelope of w_j within the specified time interval. To the same order of approximation as in the spectral correlations [c.f. Equation (12)] we can write

20

(C)

$$(\omega_0 + \mu t)\, \tau_i = 2\pi N_i + \zeta_i + \mu t \tau_i$$

$$(\omega_0 + \mu t)\, \epsilon \tau_i \simeq 2\pi N_i + \chi_i + \mu t \tau_i$$

(36)

Then, a time correlation analogous to the spectral correlation of Equation (11) is

$$R_{12}(\sigma) \simeq \mathrm{Re} \int_{-T}^{T} Z_1\!\left(t - \frac{\sigma}{2}\right) Z_2^{*}\!\left(t + \frac{\sigma}{2}\right)\, dt$$

$$\simeq 2T A_1 A_2 b' \sum_{i=0}^{M} \sum_{j=0}^{M} b_i b_j \frac{\sin \mu T(\tau_i - \tau_j)}{\mu T(\tau_i - \tau_j)} \cos\left[\frac{\mu\sigma}{2}(\tau_i + \tau_j)\right. \quad (37)$$

$$\left. - (\zeta_i - \chi_j) - \frac{\mu}{2}(\tau_i^2 - \epsilon^2 \tau_j^2)\right]$$

where $T \le T_0 - \tau_m - \sigma_{max}$ is chosen to ensure integration over a time interval where all $(M + 1)$ echo components in w_1 and w_2 are non-zero.

(C) Identifying $\Omega = \mu\sigma$ and $\Delta = 2\mu T \simeq 2\pi B_w$, if $T_0 >> \tau_m + \sigma_{max}$, $R_{12}(\sigma)$ has exactly the form of $R_{12}(\Omega)$, Equation (13), except for an additional term in the argument of the cosine function. Thus, in addition to the constraints outlined for $R_{12}(\Omega)$ in the discussion of spectral cross-correlations, there is the condition that

$$\frac{\mu}{2}\left|1 - \epsilon^2\right|\tau_i << \left|\zeta_i - \chi i\right|, \quad \text{all } i$$

(38)

to be imposed if $R_{12}(\sigma)$ is used as an approximation to the spectral correlation, $R_{12}(\Omega)$. Dividing Equation (38) by τ_i, using Equation (14), $\mu = \pi B_w / T_0$, and approximating $\left|1 + \epsilon\right| \simeq 2$, this condition reduces to

$$\frac{B_w}{f_0} << \frac{2T_0}{\tau_M}$$

(39)

for the most stringent case, $i = M$. Condition (39) indicates that the ratio of signal bandwidth to carrier frequency should be much less than the ratio of

(C)   signal duration to maximum target highlight delay, a condition which is easy to meet with LFM pulses. Condition (39) is offered as an alternative to the so-called "transient" condition of [23] which seems to be based on requiring that $\mid 1/2\ \mu\tau_m^2 \mid \leq 2\pi$, or $\mid \tau_m^2 B_w/(2T_0) \mid \leq 1$, in this notation. Though condition (39) is less restrictive, it is felt to be a more realistic indication of the errors involved in approximating the spectral correlation, $R_{12}(\Omega)$, by the time correlation, $R_{12}(\sigma)$.

(C)   Because larger receiver separations and more complex signal processing (time compression of one received signal) are required for time correlations, it is felt that the spectral correlation method is more suitable to space-time processing for target classifications on the basis of shape and aspect at long-range in the bottom bounce mode. We include time correlations of the envelopes of uncompressed LFM echoes as a special form of spectral processing in the above statement. Therefore, Section III of the report is devoted to examining the effects of bottom reflections and scattering in the specular direction upon the spectral processing for classification.

SECTION III
EFFECT OF BOTTOM BOUNCE ON TARGET CLASSIFICATION

FORMULATION OF THE BOTTOM BOUNCE TARGET CLASSIFICATION PROBLEM

(C) As the discussion of Section II has shown, it is desirable that the frequency spectrum of the signal be flat within the integration interval chosen for the frequency cross-correlation of the received signal spectra. Presumably, the transmitted signal spectrum, $S_T(\omega)$, will be chosen to have properties which approximate this condition. However, in propatating through a random inhomogeneous medium and reflecting off rough impedance boundaries, the signal spectrum undergoes filtering and spreading before arriving at the receiver. It is our purpose here to examine the nature of the filtering and spreading that the signal spectrum experiences upon reflection from the bottom, and its effect upon our ability to extract the desired target characteristics when operating in the bottom bounce mode.

(C) There are essentially two main approaches to the theory of reflection, reverberation, and scattering in random inhomogeneous media: (1) The physical approach as discussed by Chernov [4], Tatarski [5], and Laval, et al. [6], in relation to a statistically homogeneous medium characterized by a random refractive index, and by Tolstoy and Clay [7] in relation to reflections from irregular surfaces, and (2) the phenomenological approach as discussed by Ol'shevskii [8] and Middleton [9], for example, wherein the inhomogenieties are introduced as a random distribution of point scatterers in the medium. The phenomenological approach has the advantage of simplicity in handling complex geometries and the higher order statistics required for system analysis and design. However, it suffers from the inability to predict the impulse response (or equivalently, the transfer function) of the

23

(C) collection of scatterers. This must be supplied at some point by comparison of the theory with experiment. But the success or failure of sonar signal classification in the bottom bounce mode by STARLITE techniques depends on the spectral properties of the bottom transfer functions within the integration band selected for the cross-correlation of the frequency spectra of two spatially-separated received signals. We therefore choose to take the physical approach, since the basic functional form of the bottom transfer function can be determined from measurable physical properties of bottom sediments as manifested in the reflection coefficient [4].

(U) To formulate the bottom bounce problem, we follow Tolstoy and Clay [7] and use the Kirchoff radiation formula of classical diffraction theory which relates the pressure interior to a bounded medium to the pressure on the boundary and the Green's function. Let the far-field acoustic pressure at a distance r_T from the transmitter be given by

$$p_T(\vec{r}_T) = \frac{p_o d_T e^{-jk_o r_T}}{r_T} \tag{40}$$

where p_o is the source strength, d_T is the source directivity, $k_o = \omega/c_o$ is the wave number for propagation at velocity c_o, and harmonic time dependence ($\sim e^{j\omega t}$) is assumed. Referring to Figure 3, the outgoing pressure wave at the point, $\vec{r}_T^{(i)}$, resulting from reflection and scattering of p_T off the rough boundary, $z = 0$, is approximately [10]

$$p(\vec{r}_T^{(i)}) = \frac{-jp_o k_o e^{-jk_o(r_T + r_T^{(i)})}}{4\pi r_T r_T^{(i)}} \int_{-\infty}^{\infty} d\vec{\chi}_T \frac{\phi_T^{(i)2} + \gamma_T^{(i)2}}{\gamma_T^{(i)}} \tag{41}$$

$$d_T(\vec{\chi}_T) \Lambda_T(\vec{\chi}_T, \omega) e^{-jk_o(\vec{\phi}_T^{(i)} \cdot \vec{\chi}_T + \gamma_T^{(i)} \zeta_T)}$$

24
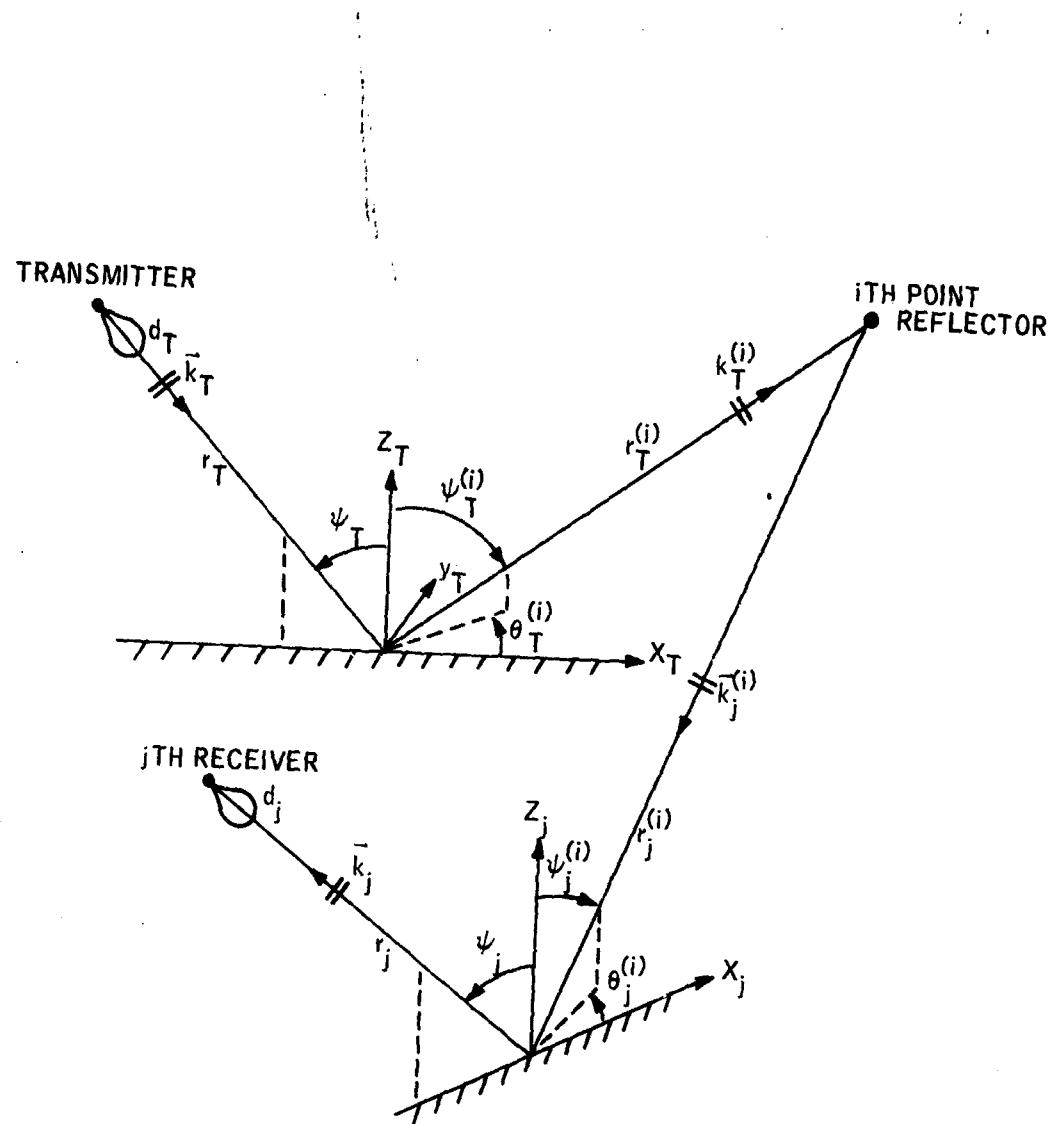
Figure 3. Geometry for Acoustic Paths in the Bottom Bounce Mode

25

where $\vec{\chi}_T = x_T\hat{i} + y_T\hat{j}$ are the coordinates of the bottom plane relative to the principal axes of the projection, $d_T(\vec{\chi}_T)$, of the source directivity function on the plane, $z = 0$, and

$$\vec{\phi}_T^{(i)} + \gamma_T^{(i)}\hat{k} = \frac{\vec{K}_T - \vec{K}_T^{(i)}}{k_o}, \quad \phi_T^{(i)} = \phi_{Tx}^{(i)}\hat{i} + \phi_{Ty}^{(i)}\hat{j} \qquad (42)$$

is a vector equal to the difference in direction cosines of the vector wave numbers for incident and reflected waves, $\zeta_T = \zeta_T(\vec{\chi}_T)$ is the random eleva-tion of the rough bottom relative to the plane, $z = 0$, and $\Lambda_T(\vec{\chi}_T, \omega)$ is the bottom reflection coefficient appropriate to the illuminated area, $d_T(\vec{\chi}_T)$.

For targets located far from the reflection point, Equation (41) can be approxi-mated by assuming that all deviations in $\vec{\phi}_T^{(i)}$ and $\gamma_T^{(i)}$ over the transmitter bottom aperture, $d_T(\vec{\chi}_T)$, from their values in the specular direction are negligible, i.e., $\phi_T^{(i)} = 0$ and $\gamma_T = 2\cos\psi_T$. In addition, the $r_T^{(i)}$ can be approximated by

$$r_T^{(i)} \simeq r_T^{(o)} + L_i\alpha_T^{(i)} \qquad (43)$$

where L_i is the distance between the first $(i = 0)$ and $(i + 1)$ (denoted by the superscript i) point reflector on the target, $L_o = 0$, and $\alpha_T^{(i)}$ is the direction cosine of reflector i relative to the specular direction of the bottom reflected signal in a coordinate system having its origin at the first point reflector. Retaining Equation (43) in the phase, but approximating $r_T^{(i)} \simeq r_T^{(o)}$ in the amplitude, Equation (41) reduces to

$$p(r_T^{(i)} \simeq \frac{-jp_o\cos\psi_T k_o e^{-jk_o[r_T + r_T^{(o)} + L_i\alpha_T^{(i)}]}}{2\pi r_T r_T^{(o)}} \int_{-\infty}^{\infty}$$

$$\qquad (44)$$

$$d\vec{\chi}_T \, d_T(\vec{\chi}_T) \, \Lambda_T(\vec{\chi}_T, \omega) e^{-jk_o\gamma_T\zeta_T}$$

26

Recognizing that the return signal emanating from the ith point reflector of scattering amplitude, a_i, at a distance, r, from the scatterer is

$$p_i(\vec{r}) = \frac{a_i p_T(\vec{r}_T^{(i)}) e^{-jk_o r}}{r} , \tag{45}$$

a second application of the Kirchoff radiation formula to the same order of approximation as Equation (44) yields for the pressure at the jth receiver

$$p_j(\vec{r}_j) = -jk_o \sum_{i=o}^{M} \frac{a_i p_T[\vec{r}_T^{(i)}] \cos \Psi_j e^{-jk_o[r_j^{(o)} + r_j + L_j \alpha_j^{(i)}]}}{2\pi r_j r_j^{(o)}} \int_{-\infty}^{\infty} d\vec{\chi}_j d_j(\vec{\chi}_j) \Lambda_j(\vec{\chi}_j, \omega) e^{-jk_o \gamma_j \zeta_j} \tag{46}$$

where subscript j on a variable denotes the same type of function as defined for Equation (44), but now as applies to the jth receiver.

Received Signal Spectra

Finally, since the response of a linear system to a simple harmonic wave is the transfer function of the system, given a transmitted signal, $s_T(t)$, with frequency spectrum, $S_T(\omega)$, the frequency spectrum, $W_j'(\omega)$, of the received signal at the jth receiver is determined by Equations (46) and (44), with p_o replaced by $S_T(\omega)$. Writing $W_j'(\omega)$ so as to explicitly indicate its frequency dependence

$$W_j'(\omega) = \omega^2 S_T(\omega) \sum_{i=o}^{M} b_i^{(j)} e^{-j\omega[t_j + \tau_i^{(j)}]} \mathcal{L}_{\vec{\chi}_T} \mathcal{L}_{\vec{\chi}_j} \left\{ d_T(\vec{\chi}_T) d_j(\vec{\chi}_j) \Lambda_T(\vec{\chi}_T, \omega) \Lambda_j(\vec{\chi}_j, \omega) e^{-j\omega(\eta_T \zeta_T + \eta_j \zeta_j)} \right\} \tag{47}$$

(U) where

$$b_i^{(j)} = \frac{-a_i \cos \Psi_T \cos \Psi_j}{(2\pi)^2 c_o^2 r_T r_T^{(o)} r_j r_j^{(o)}}$$

$$\eta_\nu = \frac{\gamma_\nu}{c_o} = \frac{2\cos \Psi_\nu}{c_o}, \qquad \nu = T \text{ or } j \qquad\qquad (48)$$

$$t_j = \frac{r_T + r_T^{(o)} + r_j + r_j^{(o)}}{c_o}$$

$$\tau_i^{(j)} = \frac{L_i}{c_o} [\alpha_T^{(i)} + \alpha_j^{(i)}]$$

and we have used the integral operator notation

$$\mathcal{L}_{\vec{\chi}} = \int_{-\infty}^{\infty} d\vec{\chi} = \int_{-\infty}^{\infty} dx \int_{-\infty}^{\infty} dy \qquad\qquad (49)$$

(C) Consider next the signals at two receivers and assume that the relative delay due to differences in the round-trip travel times, t_1 and t_2, has been removed. Defining

$$W_1(\omega) = e^{j\omega t_1} W_1'(\omega) = H_1(\omega) S_1(\omega)$$

$$\qquad\qquad (50)$$

$$W_2(\omega) = e^{j\omega t_2} W_2'(\omega) = H_2(\omega) S_2(\omega)$$

28

(C) we can write

$$H_1(\omega) = \sum_{i=0}^{M} b_i e^{-\omega \tau_i}$$

$$H_2(\omega) = b' \sum_{i=0}^{M} b_i e^{-j\omega \epsilon_i \tau_i}$$

(51)

by defining

$$b_i \equiv b_i^{(1)}$$

$$b' \equiv b_i^{(2)} \Big/ b_i^{(1)} = \frac{r_2^{(0)} r_2 \cos \Psi_2}{r_1^{(0)} r_1 \cos \Psi_1} , \text{ all } i$$

(52)

$$\tau_i = \tau_i^{(1)}$$

$$\epsilon_i = \frac{\tau_i^{(2)}}{\tau_i^{(1)}} = \frac{\alpha_T^{(i)} + \alpha_2^{(i)}}{\alpha_T^{(i)} + \alpha_1^{(i)}} , \quad i = 1, 2, \ldots, M$$

Also, the signal spectra, $S_j(\omega)$, can be written in the form

$$S_j(\omega) \equiv G_j(\omega) S_T(\omega)$$

(53)

where

$$G_j(\omega) = \omega^2 \mathcal{L}_{\vec{\chi}_T} \mathcal{L}_{\vec{\chi}_j} \left\{ d_T(\vec{\chi}_T) d_j(\vec{\chi}_j) \Lambda_T(\vec{\chi}_T, \omega) \Lambda_j(\vec{\chi}_j, \omega) e^{-j\omega(\eta_T \zeta_T + \eta_j \zeta_j)} \right\}$$ (54)

is the transfer function associated with the bottom reflections encountered by $S_T(\omega)$ in traveling to the jth receiver. It is seen by Equations (50) and (51) that the signal spectra, $W_1(\omega)$ and $W_2(\omega)$, have the desired form for performing target classification ala STARLITE, provided $S_1(\omega)$ and $S_2(\omega)$ are nearly

(C) constant over the integration interval of $R_{12}(\Omega)$. Since $S_T(\omega)$ is presumably chosen to be sufficiently flat over the interval, success or failure of the classification scheme ultimately rests on the properties of $G_j(\omega)$. Therefore, we direct our attention to the frequency dependence of these transfer functions which behave like random filters in the communication channel.

Expectation of $R_{12}(\Omega)$

(C) Because of the roughness of the bottom surface and randomness in the reflection coefficients, the statistical expectation of $R_{12}(\Omega)$ is of interest. For reasons presented later in this discussion, the frequency cross-correlation for bottom bounce operation is taken in the form

$$<R_{12}(\Omega)> = <\operatorname{Re} \int_{\omega_o - \frac{\Delta}{2}}^{\omega_o + \frac{\Delta}{2}} W_1\left(\omega - \frac{\Omega}{2}\right) W_2^*\left(\omega + \frac{\Omega}{2}\right) d_\omega >$$

$$= \operatorname{Re} \int_{\omega_o - \frac{\Delta}{2}}^{\omega_o + \frac{\Delta}{2}} H_1(\omega - \frac{\Omega}{2}) H_2^*(\omega + \frac{\Omega}{2}) S_T(\omega - \frac{\Omega}{2}) S_T^*(\omega + \frac{\Omega}{2}) \qquad (55)$$

$$<G_1(\omega - \frac{\Omega}{2}) G_2^*(\omega + \frac{\Omega}{2})> d\omega$$

where the bracket $<\ >$ denotes the statistical average over all appropriate random variables. The expectation $<G_1 G_2^*>$ includes both coherent and incoherent scattering in the specular direction from the bottom sediments. No effort is made to separate the two here, since it is the properties of $<R_{12}>$ which are of interest, not those of G_1 and G_2 in and of themselves. It is to be noted from Equation (55) that loss of coherence in the specular direction by the signal upon reflections from the boundary has no effect, per se, on the target classification scheme. All we seek is a proper vehicle for creation of

30

(C) a spectral window within which to view the properties of $H_1(\omega - \Omega/2)$ $H_2^*(\omega + \Omega/2)$. Hence, the coherence properties of the reflected signal, $S_j(\omega)$, relative to the transmitted signal, $S_T(\omega)$, are immaterial. What does matter is that S_1 and S_2 have sufficient coherent energy within the band $[\omega_o - \Delta/2, \omega_o + \Delta/2]$ to raise $\langle R_{12} \rangle$ above the reverberant and ambient noise level and that the distribution of that energy within the band be sufficiently flat so as not to obscure the target properties contained in H_1 and H_2.

(U) At ranges of the order of 20 to 40 thousand yards, one can reasonably expect essentially complete overlap of the bottom illumination functions d_T, d_1, and d_2. As a result, fourth-order statistical moments of the reflection coefficients and surface roughness are required in computing $\langle G_1 G_2^* \rangle$. This overlap is desirable, since a high degree of correlation between $S_1(\omega)$ and $S_2(\omega)$ improves the prospects for successful target classification. However, this presents complications relative to performing the spatial integrations over the bottom aperture functions when weighted by these higher-order moments. To reduce the complexity of $\langle G_1 G_2^* \rangle$, and yet preserve the essential sameness of S_1 and S_2, it will be assumed that there is no statistical dependence of the reflection coefficients and surface roughness between the outgoing and return reflections. Physically, this corresponds to a situation where there is a large separation between the transmitter and two relatively closely-spaced receivers, so that there is complete overlap of d_1 and d_2, but none between d_T and either d_1 or d_2. In addition, it will be assumed that the surface roughness is statistically independent of the reflection coefficient. The expectation $\langle G_1 G_2^* \rangle$ is then

$$
\begin{aligned}
\langle G_1(\omega - \tfrac{\Omega}{2}) G_2^*(\omega + \tfrac{\Omega}{2}) \rangle &= (\omega^2 - \tfrac{\Omega^2}{4}) \mathcal{L}_{\vec{x}_T} \mathcal{L}_{\vec{x}_T'} \Big\{ d_T(\vec{x}_T) d_T(\vec{x}_T') \langle \Lambda_T(\vec{x}_T, \omega - \tfrac{\Omega}{2}) \Lambda_T^*(\vec{x}_T', \omega + \tfrac{\Omega}{2}) \rangle \\
&\quad \cdot \langle \exp\{ -j\eta_T[(\omega - \tfrac{\Omega}{2}) \zeta_T(\vec{x}_T) - (\omega + \tfrac{\Omega}{2}) \zeta_T(\vec{x}_T')] \} \rangle \Big\} \\
&\quad \cdot (\omega^2 - \tfrac{\Omega^2}{4}) \mathcal{L}_{\vec{x}_R} \mathcal{L}_{\vec{x}_R'} \Big\{ d_R(\vec{x}_R) d_R(\vec{x}_R') \langle \Lambda_R(\vec{x}_R, \omega - \tfrac{\Omega}{2}) \Lambda_R^*(\vec{x}_R', \omega + \tfrac{\Omega}{2}) \rangle \\
&\quad \cdot \langle \exp\{ -j\eta_R[(\omega - \tfrac{\Omega}{2}) \zeta_R(\vec{x}_R) - (\omega + \tfrac{\Omega}{2}) \zeta_R(\vec{x}_R')] \} \rangle \Big\}
\end{aligned}
\tag{56}
$$

31

where it is assumed that $d_1 = d_2 = d_R$, $\eta_1 = \eta_2 = \eta_R$ and $\Lambda_1 = \Lambda_2 = \Lambda_R$. Under these assumptions, the expectation of the bottom transfer functions can be written as

$$<G_1(\omega - \frac{\Omega}{2}) \, G_2^*(\omega + \frac{\Omega}{2})> \; = I_T(\omega, \Omega) \, I_R(\omega, \Omega) \tag{57}$$

where I_T and I_R have the same functional form if d_T and d_R, Λ_T and Λ_R, and ζ_T and ζ_R each have similar functional forms and distributions. Assuming this also is the case, the problem is reduced to consideration of the integral

$$I(\omega, \Omega) = \left(\omega^2 - \frac{\Omega^2}{4} \right) \mathcal{L}_{\vec{\chi}} \mathcal{L}_{\vec{\chi}'} \left\{ \begin{array}{l} d(\vec{\chi}) d(\vec{\chi}') < \Lambda\left(\vec{\chi}, \omega - \frac{\Omega}{2}\right) \Lambda^*\left(\vec{\chi}', \omega + \frac{\Omega}{2}\right) > \\ \cdot <\exp\left\{ -j\eta\left[\left(\omega - \frac{\Omega}{2}\right)\zeta(\vec{\chi}) - \left(\omega + \frac{\Omega}{2}\right)\zeta(\vec{\chi}')\right]\right\}> \end{array} \right\} \tag{58}$$

Evaluation of $I(\omega, \Omega)$ requires specification of the bottom illumination function, $d(\vec{\chi})$, the functional form of the reflection coefficient, Λ, and the joint probability distributions of the surface roughness and random parameters in Λ. As described in Appendix A, the bottom reflection coefficient, Λ, is assumed to have the form

$$\Lambda(\chi, \omega) = \sum_{n=0}^{N} \lambda_n e^{-j\omega \sum_{q=0}^{n} \beta_q \ell_q(\chi)} \tag{59}$$

where λ_n is a reflection coefficient associated with the interface between two layers in the stratified medium, β_n is an inverse velocity associated with the wave propagation in a given layer, and ℓ_n is the layer thickness. Based on measurements of attenuation in bottom sediments, λ_n and β_n are taken to be complex constants. The randomness in Λ is assumed to be characterized by irregular layer thicknesses, ℓ_n, solely.

The details of the evaluation of $I(\omega, \Omega)$ under the assumptions of a gaussian illumination function and joint gaussian distributions for ζ and ℓ are carried out in Appendix B. The result for these and other assumptions made in the course of the analysis is that

$$I(\omega, \Omega) \simeq (\omega^2 - \frac{\Omega^2}{4})e^{-\eta^2 \sigma_\zeta^2 (\omega^2 + \frac{\Omega^2}{4})} \sum_{n=0}^{N} \sum_{m=0}^{N} \lambda_n \lambda_m^* J_{nm}(\omega, \Omega) \qquad (60)$$

$$\cdot e^{-j(\omega - \frac{\Omega}{2})\mu_n + j(\omega + \frac{\Omega}{2})\mu_m^* - \frac{1}{2}(\omega - \frac{\Omega}{2})^2 \varkappa_n - \frac{1}{2}(\omega + \frac{\Omega}{2})^2 \varkappa_m^*}$$

where

$$\left. \begin{aligned} \mu_n &= \sum_{q=0}^{n} \beta_q \bar{\ell}_q \\[2em] \varkappa_n &= \sum_{q=0}^{n} \sum_{p=0}^{n} \beta_q \beta_p \sigma_{qp}^2 \end{aligned} \right\} \qquad (61)$$

and

$$J_{nm}(\omega, \Omega) = (2\pi DxDy)^2 + \frac{2\pi^2 DxDy Lx_{nm} Ly_{nm}}{\sqrt{1 - a_{nm}^2}} \left\{ \begin{aligned} &\bar{E}_i\left[\left(\omega^2 - \frac{\Omega^2}{4} \right) t_{nm}^2 \right] \\ &-\gamma_E - \ell_n\left[\left(\omega^2 - \frac{\Omega^2}{4} \right) t_{nm}^2 \right] \end{aligned} \right\} (62)$$

In addition, $\bar{\ell}_q$ is the mean of ℓ_q, σ_{qp}^2 is the covariance of $\ell_q(\vec{\chi})$ and $\ell_p(\vec{\chi})$, σ_ζ^2 is the variance of $\zeta(\vec{\chi})$, Dx and Dy are characteristic lengths associated with the principal axes of $d(\vec{\chi})$, Lx_{nm} and Ly_{nm} are correlation lengths associated with a composite spatial correlation coefficient, $\tilde{\rho}_{nm}(\vec{\chi}, \vec{\chi'})$, defined by Equations (B15) and (B17), along the principal axes of $d_T(\vec{\chi})$, a_{nm} is a coefficient associated with the transformation of the correlation lengths appropriate to the principal axes of $\tilde{\rho}_{nm}$ into Lx_{nm} and Ly_{nm}, $E_i(x)$ is the exponential integral as defined in Equation (B25), γ_E is Euler's constant, and finally

$$t_{nm}^2 = \eta^2 \sigma_\zeta^2 + \sum_{q, p = 0}^{\min(n, m)} \sigma_{qp}^2 \, \text{Re}(\beta_q \beta_p^*) \qquad (63)$$

33

SPECTRAL PROPERTIES OF BOTTOM TRANSFER FUNCTION

(C) The ultimate purpose of this investigation would be to examine $<R_{12}(\Omega)>$ in the vicinity of its maximum at a frequency shift, $\hat{\Omega}$, in order to estimate how much deviation from the desired condition, $\hat{\Omega} = (1-\epsilon)\omega_o$, is encountered in the bottom bounce mode of operation when the target is a line target. In addition, one would like to design the transmitted signal spectrum, $S_T(\omega)$, so as to compensate for errors in $\hat{\Omega}$ introduced by bottom reflections. Because of the complexity in the integral in Equation (55) and the uncertainty in the acoustic parameters characterizing the bottom sediments over a variety of bottom types, such an investigation requires an extensive computer simulation of the bottom bounce classification problem. Unfortunately, a computer simulation of this magnitude was not within the scope of the present contract.

Smooth Boundaries

(C) Some light can be shed on the possibilities for success of the STARLITE classification scheme in the bottom bounce mode by examining the frequency dependence of $I(\omega, \Omega)$ in the vicinity of the carrier frequency, ω_o, since, ideally, $I(\omega, \Omega)$ would be flat over the interval $[\omega_o - \Delta/2, \ \omega_o + \Delta/2]$ and independent of the frequency shift, Ω. For a nearly smooth, regular, stratified impedance boundary, such that $\omega_o t_{nm} << 1$, coherent reflections dominate and

$$I(\omega, \Omega) \sim (2\pi DxDy)^2 (\omega^2 - \frac{\Omega^2}{4}) \sum_{n,\, m=0}^{N} \lambda_n \lambda_m \, e^{\frac{\Omega}{2}(\mu_n{}^i - \mu_m{}^i) - \omega(\mu_n{}^i + \mu_m{}^i) + j\frac{\Omega}{2}(\mu_n{}^r + \mu_m{}^r) - j\omega(\mu_n{}^r - \mu_m{}^r)} \tag{64}$$

where the real and imaginary parts of the exponent have been exposed by writing

$$\mu_n = \mu_n{}^r - j\mu_n{}^i = \sum_{q=0}^{n} \beta_q{}^r \bar{\ell}_q - j \sum_{q=0}^{n} \beta_q{}^i \bar{\ell}_q \tag{65}$$

34

(C) Consider first the diagonal terms in the double sum of Equation (64). For $m = n$, the exponent in the addend reduces to $(-2\omega\mu_n^i + j\Omega\mu_n^r)$. Removal of the term $1/2 \Omega (\mu_n^i - \mu_m^i)$, for the diagonal terms at least, is the reason why the average of $W_1(\omega - \Omega/2) W_2^*(\omega + \Omega/2)$ was chosen for the cross-correlation of the frequency spectra, since this term potentially generates a strong amplitude dependence on Ω if an unsymmetric frequency shift, such as in $W_1(\omega - \Omega) W_2^*(\omega)$, is chosen for the average. The cancellation of this term and the oscillatory term, $-j\omega(\mu_n^r - \mu_m^r)$, when $m = n$ also depends on overlap of the receiver illumination functions d_1 and d_2; hence the desirability of this condition.

(C) The term, $j\Omega\mu_n^r$, introduces additional delays, μ_n^r, to the target-induced delays, τ_1. However, these delays are expected to be small compared with significant target-induced delays at large ranges for the following reasons. Reduction of data taken by Mackenzie [11], and by Nuttal and Cron [12] indicates that $0.2 \tilde{>} c_o\beta_1^r \tilde{>} 0.06$ and $0.2 \tilde{<} c_o\beta_1^i \tilde{<} 1$ for angles of incidence in the range $60 \tilde{<} \Psi \le 90°$. Also, penetration depths of less than 2 m are expected for these angles of incidence [12]. Assuming that the reflection coefficient model of Equation (A14) holds, and that no more than five internal reflections within the top sediment layer are significant, $\mu_n^r < (5)\left|\dfrac{0.2}{c_o}\right|(2) \sim 1$ msec might be expected. However, the discussion of Section II indicates that significant target delays measurable by STARLITE techniques are greater than 10 msec, roughly.

(C) The condition, $\Omega \ll \Delta \ll \omega_o$, ensures that $\omega^2 - \Omega^2/4 \simeq \omega^2$. Thus, the essential ω dependence of the diagonal terms in Equation (64) reduces to functions of the form $\omega^2 \exp(-2\omega\mu_n^i)$. Recall that $\beta_o = 0$, by definition; hence, the first term in the sum is $\sim \omega^2$ while terms for $n \ge 1$ have maxima at $\omega_n = (\mu_n^i)^{-1}$. For $0.2 \tilde{\le} c_o\beta_1^i \tilde{\le} 1$, these maxima occur at frequencies $\omega_n \tilde{<} 7.5 \times 10^3$ sec^{-1}. Thus, at carrier frequencies of $f_o > 1$ KHz, the spectrum, $I(\omega, \Omega)$, is certainly not flat. Therefore, it is necessary to rely on the condition $\Delta \ll \omega_o$ to preserve a semblance of flatness for $I(\omega, \Omega)$ in the integration interval $[\omega_o - \Delta/2, \omega_o + \Delta/2]$.

(C) With regard to the off-diagonal terms, $m \neq n$, in Equation (64), it is reasonable to expect that if $\exp[1/2\Omega(\mu_n^i - \mu_m^i)]$ is significantly different from unity, then $\exp[-\omega(\mu_n^i + \mu_m^i)]$ is much smaller than a comparable diagonal term $\exp[-2\omega\mu_n^i]$, and therefore, such off-diagonal terms are negligible. Off-diagonal terms that are not negligible in comparison with like diagonal terms require that $\Delta(\mu_n^r - \mu_m^r) \ll 1$ in order that $I(\omega, \Omega)$ not be too oscillatory over the integration band.

Rough Surfaces

(C) Next we consider the effect of surface roughness by assuming that $\omega_0 \eta \sigma_\zeta \gg 1$, but that the σ_{qp}^2 are sufficiently small to neglect the $\varkappa_n$. Then, $t_{nm}^2 \simeq \eta^2 \sigma_\zeta^2$ and the exponential integral in J_{nm} takes on its asymtotic value and dominates the logarithmic term. If $(L/D)^2 \bar{E}_i \ll 1$ by virtue of short correlation lengths L,

$$I(\omega, \Omega) \simeq \text{const} \cdot \omega^2 e^{-\eta^2 \sigma_\zeta^2 \left(\omega^2 + \frac{\Omega^2}{4}\right)} \sum_{n, m=0}^{N} \lambda_n \lambda_m^* e^{-j\left(\omega - \frac{\Omega}{2}\right)\mu_n + j\left(\omega + \frac{\Omega}{2}\right)\mu_m^*} \quad (66)$$

If $(L/D)^2 \bar{E}_i \gg 1$,

$$I(\omega, \Omega) \simeq \text{const} \cdot e^{-\frac{1}{2}\eta^2 \sigma_\zeta^2 \Omega^2} \sum_{n, m=0}^{N} \lambda_n \lambda_m^* e^{-j\left(\omega - \frac{\Omega}{2}\right)\mu_n + j\left(\omega + \frac{\Omega}{2}\right)\mu_m^*} \quad (67)$$

In either case, $\eta^2 \sigma_\zeta^2 \Omega^2 \ll 1$ is required if a strong amplitude dependence on Ω is to be avoided. Measurements of σ_ζ in the Hatteras Abyssal plain indicate that $\sigma_\zeta < 0.5$ m in this region [13]. At incident angles $\Psi \geq 60°$ and $\sigma_\zeta \leq 0.5$ m, $\Omega^2 \sigma_\zeta^2 \eta^2 \leq 0.1$ for $\Omega \leq 900$. This is well within the range of frequency shifts for which the STARLITE method is applicable. It is also to be noted from Equations (66) and (67) that the ω dependence of $I(\omega, \Omega)$ is strongly affected by the surface roughness and its correlation lengths relative to the dimensions

(C) of the illuminated surface. In fact, rough surfaces with long correlation lengths, Equation (67), more closely approximate the desired flat frequency spectrum of $I(\omega, \Omega)$ than do smooth surfaces, Equation (64).

Irregular Sediment Layers

(U) Lastly, we consider briefly the effect of irregularities in the sediment layer thicknesses on $I(\omega, \Omega)$. Defining

$$\varkappa_n = \varkappa_n{}^r - j\varkappa_n{}^i \equiv \sum_{q,p=o}^{n} (\beta_q{}^r \beta_1{}^r - \beta_q{}^i \beta_p{}^i)\sigma_{qp}{}^2 - j \sum_{q,p=o}^{n} (\beta_q{}^r \beta_p{}^i + \beta_p{}^r)\sigma_{qp}{}^2 \quad (68)$$

the exponent of interest is of the form

$$X = -\frac{1}{2}\left(\omega - \frac{\Omega}{2}\right)^2 \varkappa_n - \frac{1}{2}\left(\omega + \frac{\Omega}{2}\right)^2 \varkappa_m{}^* = -\frac{1}{2}\left(\omega^2 + \frac{\Omega^2}{4}\right)\left(\varkappa_n{}^r + \varkappa_m{}^r\right)$$
$$+ \frac{\omega\Omega}{2}\left(\varkappa_n{}^r - \varkappa_m{}^r\right) + j\frac{1}{2}\left[\left(\omega^2 + \frac{\Omega^2}{4}\right)\left(\varkappa_m{}^i - \varkappa_m{}^i\right) - \omega\Omega\left(\varkappa_n{}^i + \varkappa_m{}^i\right)\right] \quad (69)$$

Again, consider the case of incident angles near and above critical, and assume that essentially only the top layer is penetrated, so $\beta_n = \beta_1$ for all n. Near critical incidence, $\beta_1{}^r \approx \beta_1{}^i$, so $\varkappa_n{}^r \approx 0$. However, above critical incidence, $\beta_1{}^i > \beta_1{}^r$ and $\varkappa_n{}^r < 0$. This creates terms of the form $\exp(+\omega^2 |\varkappa^r|)$ in $I(\omega, \Omega)$ which tend to compensate for the negative slope of terms of the form $\exp(-\omega\mu^i)$. The terms $1/2\omega\Omega (\varkappa_n{}^r - \varkappa_m{}^r)$ and $1/2 j (\omega^2 + \Omega^2/4)(\varkappa_n{}^i - \varkappa_m{}^i)$ in X drop out in the diagonal elements of the double sum.

(C) To estimate the effect of the term, $1/4 \Omega^2 |\varkappa_n{}^r|$, in X, consider incident angles near grazing and assume that $c_o\beta_1{}^i \approx 1$, $\beta_1{}^r \approx 0.06/c_o$, and that no more than five internal reflections are significant as before. Then, if $\Omega \leq 600 \sec^{-1}$, $1/4 \Omega^2 |\varkappa_5{}^r| \leq 0.1$ if $\sigma_{11} \lesssim 0.3$ m. This value of σ_{11} is comparable with the value of σ_ζ quoted for the Hatteras Abyssal Plain. It therefore appears that if the surface is not too rough for STARLITE, neither will the

(C) sediment layers be too irregular. The remaining term, $-1/2\ j\omega\Omega(\varkappa_n{}^i + \varkappa_m{}^i)$, in X may be troublesome, however, since under the above conditions of near grazing incidence, $\omega\Omega\varkappa_5{}^i \stackrel{\sim}{<} 4 \times 10^{-5}\ \omega$, which is not necessarily small for carrier frequencies of $f_o > 1$ KHz.

(C) From this brief and somewhat superficial discussion of the properties of $I(\omega, \Omega)$, it seems reasonable to conclude that there is some justification for believing that STARLITE techniques are applicable to signal classification in the bottom bounce mode of operation. The conditions for operation at long range appear to be most favorable, since the effects of surface roughness and penetration of the sediment layers by the acoustic wave are reduced at angles approaching grazing incidence. However, the degree of confidence in success that one would like before initiating costly sea trials for verification of the classification method has not been achieved in this study. More extensive analysis of the properties of $<R_{12}(\Omega)>$, Equation (55), as a function of geometry, signal spectrum, and parameters of the bottom transfer functions through computer simulation is expected to provide a higher confidence estimate of the probability of success of bottom bounce STARLITE. In addition, the effects of target and transmitter-receiver motion, ocean surface backscatter, volume and surface reverberation, ambient noise, and scattering off corrugated surfaces should also be studied before final judgment is passed on the theoretical practicality of bottom bounce STARLITE.

38

SECTION IV
CONCLUSIONS AND RECOMMENDATIONS

(C) To establish direction to this study of sonar signal characteristics in the bottom bounce mode, it was decided to concentrate on the effects of bottom reflections as related to target classification on the basis of shape and aspect for targets characterized as arrays of point scatterers. A review of the general theoretical requirements for target shape and aspect classification through spectral and time cross-correlations of signals received at two different space points has indicated that:*

1) Spectral processing is more promising than time processing for shape and aspect classification from a practical point of view, since considerably larger receiver separations are required for time correlations (of the order of the ratio of the signal carrier frequency to the bandwidth, f_0 / B_w, times larger). We identify the special case of time cross-correlation of the envelopes of uncompressed linear FM signals with spectral processing in this observation.

2) A band-limited spectral cross-correlation with symmetric frequency shifts of the form

$$R_{12}(\Omega) = \text{Re} \int_{\omega_0 - \frac{\Delta}{2}}^{\omega_0 + \frac{\Delta}{2}} W_1(\omega - \frac{\Omega}{2})\ W_2^*(\omega + \frac{\Omega}{2})\ d\omega$$

---

*The authors regret that they were unable to obtain a copy of the report "An Experimental Study of STARLITE using a Scaled AN/SQQ-23 (PAIR) Configuration," DRL-TM-68-10 (AD 390 245L), in time to influence this theoretical study.

should be used for spectral processing to confine the observation of the target transfer function to the interior of the spectral window created by the transmitted signal and negate the errors in estimating target aspect introduced by attenuation in bottom reflections.

3) Geometric and signal parameter constraints for spectral processing are somewhat different, and more restrictive in the case of the correlation and ambiguity conditions, but less restrictive in the case of the resolution and transient conditions, than indicated in the original STARLITE analysis [2], [23] of spectral processing.

4) Large f_0 and B_w are desirable for satisfying spectral processing constraints with reasonable receiver separations, whereas low f_0 and small B_w are desirable to minimize propagation loss and distortion of the spectral window in bottom reflections. Therefore, optimum f_0 and B_w depend upon target range and bottom conditions.

5) An example for f_0 = 6 KHz and B_w = 600 Hz indicated that receiver separations, D, of about 175 yards permitted classification over line target aspect angles of $15° \leq \omega \leq 60°$ and $120° \leq \omega \leq 165°$ (bear sp ct at 0° and 180°, bow or stern aspect at 90° in this nutation) for a target of length L_m = 90 m at a bearing θ = 90° and ranges of 20 to 40 thousand yards. However, since D is inversely proportional to L_m, f_0, and $\sin \theta$, reduction of any of these parameters requires a corresponding increase in D to maintain classification over the same interval of ranges and aspect angles. It therefore appears that some flexibility in selecting receiver separations as a function of range and bearing is necessary.

40

(C) With regard to the feasibility of STARLITE processing in the bottom bounce mode, our conclusions are somewhat more tentative. A physical approach to the modeling of sonar wave reflections off an irregular impedance boundary [7] has been taken in the analysis in order that the frequency dependance of the bottom transfer function can be related to measurable physical properties of the bottom sediments. The analysis requires a considerable degree of approximation and a number of assumptions to obtain analytically tractable results. However, comparisons of similar analytic developments with controlled experiments indicate that the assumptions and approximations are perhaps not too restrictive as applied to this type of problem [7]:

1) STARLITE signal processing concepts indicate that the ideal bottom transfer function would be independent of frequency within the interval chosen for spectral cross-correlation. However, it has been shown that the spectral properties of the bottom transfer function can vary widely (low-pass, high-pass, bandpass, or notched-filter shape) depending upon f_0, B_w, angle of incidence, the degree of surface roughness, irregularities in the sediment layer thicknesses, and the amount of attenuation associated with the sediment layers.

2) In spite of the complexity of the bottom transfer function, a cursory examination of its frequency dependence for parameter values typical of the abyssal plains leads to the conclusion that long-range bottom bounce STARLITE could be practical, since the effects of surface roughness and penetration of the boundary by the acoustic wave are minimized as the incident angle approaches grazing incidence.

(U) Because of the large number of parameters which characterize the classification problem in the bottom bounce mode, and the uncertainity in their

41

values and distributions, a parametric study through computer simulation of the classification scheme is a recommended step before the expense of verifying bottom bounce STARLITE classification techniques through special sea trials could be justified. Such a simulation would not require the many assumptions and approximations required in the present study and would:

1) Establish theoretically whether or not bottom bounce STARLITE classification concepts are feasible.

2) Provide valuable guides to possible future experiments at sea by determining optimal signal carrier frequencies and bandwidths, and parameter constraints that are realistic to the bottom bounce mode of operation.

APPENDIX A
BOTTOM REFLECTION COEFFICIENT MODEL

The basic model for the ocean bottom is a regular stratified medium as shown in Figure A1. All layered media are assumed to be absorbing, and for the moment, separated by plane boundaries. The bottom is assumed to consist of N layers of finite thickness, ℓ_n, $1 \leq n \leq N$, overlying an absorbing, semi-infinite supporting half-space (medium $N + 1$). The ocean is defined to be the oth medium and is assumed to be a semi-infinite, nonabsorbing fluid. We define the nth interface to be the boundary between the nth and $(n + 1)^{th}$ media.

From wave impedance concepts for plane waves with harmonic time dependence ($\sim e^{j\omega t}$), the reflection coefficient at the nth interface for obliquely incident waves is given by [14]:

$$\Lambda_n = \frac{\hat{\lambda}_n + \Lambda_{n+1} e^{-j\omega \hat{\beta}_{n+1} \ell_{n+1}}}{1 + \hat{\lambda}_n \Lambda_{n+1} e^{-j\omega \hat{\beta}_{n+1} \ell_{n+1}}} \tag{A1}$$

In Equation (A1), Λ_n is interpretable as the reflection coefficient at the nth interface for waves impinging on the $(n + 1)^{st}$ to $(N + 1)^{st}$ media when the nth medium is considered to be semi-infinite, $\hat{\lambda}_n$ is the reflection coefficient at the nth interface when <u>both</u> the nth and $(n + 1)^{st}$ media are considered to be semi-infinite, and $\hat{\beta}_n^{-1}$ is one-half the normal component of the complex phase velocity of the wave propagating in the nth layer.

To relate $\hat{\lambda}_n$ and $\hat{\beta}_n$ to acoustical properties of the media, consider, for example, plane wave propagation in an absorbing fluid for which the Naviar-Stokes and continuity equations take the following form:

43
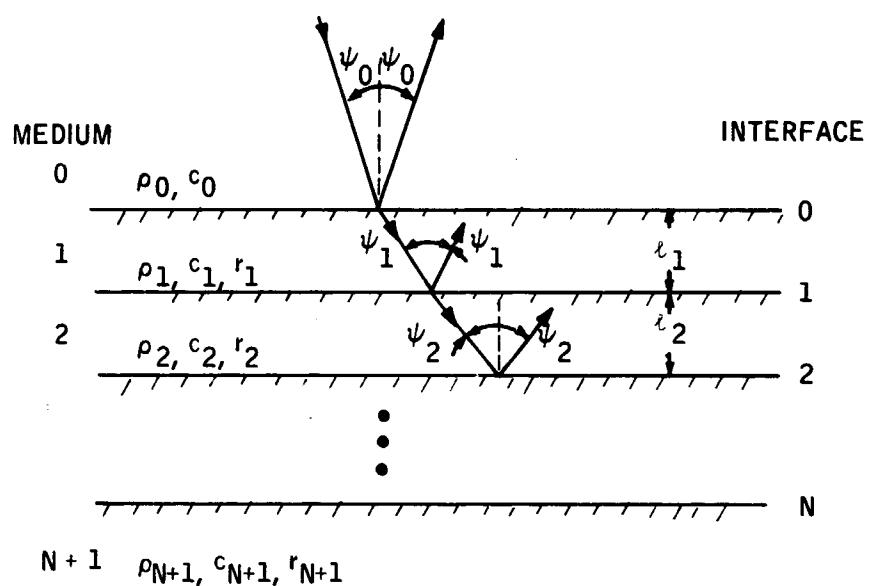
Figure A1. Geometry for a Regular Stratified Bottom

44

$$\frac{\partial \vec{u}_n}{\partial t} + r_n \vec{u}_n + \frac{1}{\rho_n} \text{grad } p_n = 0$$

(A2)

$$\frac{1}{c_n^2} \frac{\partial p_n}{\partial t} + \rho_n \text{ div } \vec{u}_n = 0$$

In these equations, p_n is the pressure, $\vec{u}_n$ the vector particle velocity, ρ_n the fluid density, r_n the normalized acoustic flow resistivity, and c_n the phase velocity in the limit, $r_n \to 0$. The intrinsic impedance, $\hat{z}_n$, of a medium characterized by Equation (A2) is

$$\hat{z}_n = \rho_n c_n \sqrt{1 - j\, r_n/\omega}$$

(A3)

and the complex wave number for harmonic plane waves is

$$k_n = \frac{\omega}{c_n} \sqrt{1 - j\, r_n/\omega}$$

(A4)

For a plane wave incident from the 0th medium at a (real) velocity, c_o, and angle, Ψ_o, Snell's law yields

$$k_n \sin \Psi_n = k_o \sin \Psi_o$$

(A5)

where $k_o = \omega/c_o$. From Equations (A4) and (A5), the cosine of the (complex) angle of incidence, Ψ_n, at the nth interface is

$$\cos \Psi_n = \sqrt{1 - \frac{c_n^2}{c_o} \frac{\sin^2 \Psi_o}{\left(1 - j\, \dfrac{r_n}{\omega}\right)}}$$

(A6)

45

Since the complex phase velocity in the nth medium is k_n/ω, from Equations (A4) and (A6) and the definition of $\hat{\beta}_n$

$$\hat{\beta}_n = \frac{2 \cos \Psi_n}{(k_n/\omega)} = 2\sqrt{\frac{(1 - j\, r_n/\omega)}{c_n^2} - \frac{\sin^2 \Psi_o}{c_o^2}} \tag{A7}$$

Finally, in terms of the normal wave impedance, z_n, the complex reflection coefficient, $\hat{\lambda}_n$, is given by [14]

$$\hat{\lambda}_n = \frac{z_{n+1} - z_n}{z_{n+1} + z_n} \tag{A8}$$

where

$$z_n = \frac{\hat{z}_n}{\cos \Psi_n} = \frac{2\rho_n (1 - j\, r_n/\omega)}{\hat{\beta}_n} \tag{A9}$$

For future reference, we note that physically, $r_n > 0$. Thus, by Equation (A7), $\hat{\beta}_n$ is of the form

$$\hat{\beta}_n = \hat{\beta}_n{}^r - j\hat{\beta}_n{}^i, \quad \hat{\beta}_n{}^r > 0, \quad \hat{\beta}_n{}^i > 0 \tag{A10}$$

for positive frequency, $\omega > 0$, $0 < \Psi_o < 90^o$, and any finite ratio of velocities, c_n/c_o.

The recursion relation, Equation (A1), terminates on the condition, $\Lambda_N = \hat{\lambda}_N$, and in principle, can be used to generate a closed-form solution for the desired reflection coefficient at the bottom, Λ_o. However, in practice we shall have to be content with a series expansion of Λ_o carried to some acceptable order of accuracy in powers of $\hat{\lambda}_n$ or $\exp(-\omega\hat{\beta}_n{}^i \ell_n)$. To determine the nature of these expansions, consider briefly some properties of

bottom sediments and the bottom reflection coefficient as determined from bottom reflectivity experiments [15, 16]. Measurements of the acoustic properties of bottom sediments indicate that the sediments near the water interface have nearly the same speed of sound as water and that the velocity and density tend to increase with depth. Adjacent sediment layers seem to have nearly the same intrinsic acoustic impedance, so that for near normal incidence, $\hat{\lambda}_n << 1$. A series expansion of Equation (A1) is of the form

$$\Lambda_n = \left(\hat{\lambda}_n + \Lambda_{n+1} e^{-j\omega\hat{\beta}_{n+1}\ell_{n+1}}\right) \sum_{m=0}^{\infty}$$

$$(-\hat{\lambda}_n \Lambda_{n+1})^m e^{-jm\omega\hat{\beta}_{n+1}\ell_{n+1}} \tag{A11}$$

which indicates that to second-order in $\hat{\lambda}_n$, Λ_n is linear in $\hat{\lambda}_n$. That is,

$$\Lambda_n^{(2)} \simeq \hat{\lambda}_n + \Lambda_{n+1} e^{-j\omega\hat{\beta}_{n+1}\ell_{n+1}} =$$

$$e^{-j\omega\hat{\beta}_n} \sum_{k=0}^{N-n} \hat{\lambda}_{n+k} e^{-j\omega \sum_{q=0}^{k} \hat{\beta}_{n+q}\ell_{n+q}} \tag{A12}$$

and, in particular,

$$\Lambda_o^{(2)} \simeq \sum_{n=0}^{N} \hat{\lambda}_n e^{-j\omega \sum_{q=0}^{n} \hat{\beta}_q \ell_q} \tag{A13}$$

where $\hat{\beta} \equiv 0$. Bottom reflectivity measurements in [16] indicate that $\Lambda_o < 0.4$ for incident angles of $\Psi_o < 60^{\circ}$. Since the acoustic wave penetration of the boundary was apparently quite deep, and encompassed several acoustically distinct sediment layers, one expects that the $\hat{\lambda}_n$ for these measurements were somewhat smaller than Λ_o and that the approximation of Equation (A13) would hold over this range of Ψ_o.

Measurements of the reflection coefficient [16] over the range $60° < \psi_o < 90°$ indicated that the penetration of the bottom by the acoustic wave was quite shallow ($\tilde{<} 2$ m). If we assume that essentially only one sediment layer is penetrated at angles near and above critical incidence, from Equation (A1), with $\Lambda_1 = \hat{\lambda}_1$,

$$\Lambda_o = (\hat{\lambda}_o + \hat{\lambda}_1 e^{-j\omega\hat{\beta}_1 \ell_1}) \sum_{n=o}^{\infty} (-\hat{\lambda}_o \hat{\lambda}_1)^n e^{-jn\omega\hat{\beta}_1 \ell_1} \tag{A14}$$

The series in Equation (A14) can be terminated after $\tilde{N}$ terms when $\tilde{N}\omega\hat{\beta}_1^i \ell_1$ is sufficiently large and the equation written in the same form as Equation (A13), i.e.,

$$\Lambda_o \simeq \sum_{n=o}^{\tilde{N}} \tilde{\lambda}_n e^{-j\omega \sum_{q=o}^{n} \tilde{\beta}_q \tilde{\ell}_q} \tag{A15}$$

where

$$\tilde{\lambda}_o = \hat{\lambda}_o$$

$$\tilde{\lambda}_n = \hat{\lambda}^{n+1}(-\hat{\lambda}_1)^n + (-\hat{\lambda}_o)^{n-1}(\lambda_1)^n, \quad n > 1$$

$$\tilde{\beta}_o = 0; \tilde{\beta}_q = \hat{\beta}_1, \quad q = 1, \dots, n \tag{A16}$$

$$\tilde{\ell}_q = \ell_1$$

For the purposes of the discussions in this report, then, it will be assumed that the bottom reflection coefficient, Λ, is adequately described by a function of the form

$$\Lambda = \sum_{n=o}^{N} \lambda_n e^{-j\omega \sum_{q=o}^{n} \beta_q \ell_q} \tag{A17}$$

where $\beta_o \equiv 0$, $\lambda_n = \hat{\lambda}_n$ or $\tilde{\lambda}_n$ and $\beta_q = \hat{\beta}_q$ or $\tilde{\beta}_q$, whichever is appropriate to the angle of incidence, ψ_o.

Since Λ is an important contributer to the transfer function representing bottom reflections, the frequency dependence and randomness of the parameters describing Λ are of interest. With regard to the frequency dependence, measurements of attenuation in bottom sediments indicate that it is a linear function of frequency [12, 17, 18, 19]. For fluid-like sediments describable by Equation (A2), this implies that the $\hat{\beta}_n$ are independent of frequency, and hence that r_n/ω = constant. Therefore, by Equations (A8) and (A9), the $\hat{\lambda}_n$ are also independent of frequency. With regard to randomness in the reflection coefficient over the area illuminated by the transmitter and receiver, inhomogenities in the sediments can create variations in the density and phase velocity of the media, where uneven deposition of sediments gives rise to variations in the layer thicknesses and mixing of sediments at the boundaries, thus making it difficult to distinguish a precise boundary. Therefore, it is expected that the quantities λ_n, β_n, and ℓ_n are best described by random functions of the spatial coordinates of the bottom, but not time. However, for simplicity, we will ignore any possible randomness in λ_n and β_n, thereby assuming that the essential nature of the randomness in Λ is contained in the layer thicknesses, ℓ_n. In summary, the model chosen for the bottom reflection coefficient is that of Equation (A17), where λ_n and β_n are complex constants and ℓ_n is a real, random function of the bottom coordinates.

49

APPENDIX B
EVALUATION OF THE INTEGRAL, $I(\omega, \Omega)$

In this appendix, we consider a solution of the integral

$$I(\omega, \Omega) = \left(\omega^2 - \frac{\Omega^2}{4}\right) \mathcal{L}_{\vec{\chi}} \mathcal{L}_{\vec{\chi}'} \left\{ \int d(\vec{\chi}) d(\vec{\chi}') < \Lambda\left(\vec{\chi}, \omega - \frac{\Omega}{2}\right) \Lambda^*\left(\vec{\chi}', \omega + \frac{\Omega}{2}\right) > < e^{-j\eta\left[\left(\omega - \frac{\Omega}{2}\right) \zeta(\vec{\chi}) - \left(\omega + \frac{\Omega}{2}\right) \zeta(\vec{\chi}')\right]} > \right\} \quad (B1)$$

under the assumptions that:

1) The bottom apertures are gaussian illumination functions:

$$d(\vec{\chi}) = d(x, y) = \exp\left[-\frac{1}{2}\left(\frac{x^2}{Dx^2} + \frac{y^2}{Dy^2}\right)\right] \quad (B2)$$

2) The reflection c efficients have the form stipulated in
    Appendix A:

$$\Lambda(\vec{\chi}, \omega) = \sum_{n=0}^{N} \lambda_n e^{-j\omega \sum_{q=0}^{n} \beta_q \ell_q(\vec{\chi})} \quad (B3)$$

3) The sediment layer thicknesses, $\ell_q(\vec{\chi})$, and surface roughness,
    $\zeta(\vec{\chi})$, are gaussian random variables with homogeneous correla-
    tion coefficients. More explicitly, for

$$\vec{\chi} - \vec{\chi}' = (x - x') \hat{i} + (y - y') \hat{j} \equiv u\hat{i} + v\hat{j} \quad (B4)$$

50

it is assumed that

$$<\zeta(\vec{\chi})> = 0$$

$$<\zeta(\vec{\chi})\, \zeta(\vec{\chi}')> = \sigma_\zeta^2\, \rho_\zeta(u, v)$$

$$\sigma_\zeta^2 = <\zeta^2(\vec{\chi})>$$

$$\rho_\zeta(0, 0) = 1$$

$$\quad\text{(B5)}$$

and

$$<\ell_q(\vec{\chi})> = \bar{\ell}_q$$

$$<\ell_q(\vec{\chi})\, \ell_p(\vec{\chi}')> = \sigma_{qp}^2\, \rho_{qp}(u, v)$$

$$\rho_{qp} = \rho_{pq}, \quad \rho_{qp}(0, 0) = 1$$

$$0 \le \sigma_{qp}^2 \le \sigma_{pq}^2 = <(\ell_q - \bar{\ell}_q)^2>$$

$$\quad\text{(B6)}$$

In the notation of Equations (B5) and (B6), σ^2 is a variance and ρ is a normalized spatial correlation coefficient. The variance, $\sigma_{qp}^2 \le \sigma_{qq}^2$, is specified, since different sediment layer thicknesses at the same place do not, in general, correlate perfectly.

Denoting $\zeta(\vec{\chi}')$ and $\ell_q(\vec{\chi}')$ by ζ' and ℓ_q', respectively, $I(\omega, \Omega)$ takes the form

$$I(\omega, \Omega) = \left(\omega^2 - \frac{\Omega^2}{4}\right)\sum_{n=o}^{N}\sum_{m=o}^{N}\lambda_n\lambda_m^*\, \mathcal{L}_{\vec{\chi}\vec{\chi}'}$$

$$\left\{ d(\vec{\chi})d(\vec{\chi}') <e^{-jn\left[\left(\omega - \frac{\Omega}{2}\right)\zeta - \left(\omega + \frac{\Omega}{2}\right)\zeta'\right]}> \right.$$

$$\left. \cdot <e^{-j\left[\left(\omega - \frac{\Omega}{2}\right)\sum_{q=o}^{n}\beta_q\ell_q - \left(\omega + \frac{\Omega}{2}\right)\sum_{p=o}^{m}\beta_p^*\ell_p'\right]}> \right\}$$

$$\quad\text{(B7)}$$

51

It is well known that the joint characteristic function, $\Psi_{\underline{z}}(\nu)$, of a vector gaussian variable, $\underline{z}$, $\underline{z}^t = [z_1, z_2, \ldots, z_n]$, is [20]:

$$\Psi_{\underline{z}}(\nu) = \langle e^{-j\underline{\nu}^t \underline{z}} \rangle = e^{-j\underline{\nu}^t \bar{\underline{z}} - \frac{1}{2}\underline{\nu}^t K_{\underline{z}} \underline{\nu}} \qquad (B8)$$

where $\underline{\nu}$ is an n-dimensional column vector, t denotes the transpose, $\bar{\underline{z}}$ is the mean of $\underline{z}$, and $K_{\underline{z}}$ is the correlation matrix

$$K_{\underline{z}} = \langle (\underline{z} - \bar{\underline{z}})(\underline{z} - \bar{\underline{z}})^t \rangle \qquad (B9)$$

Since every expectation in $I(\omega, \Omega)$ is of the form of Ψ, we can write

$$I(\omega, \Omega) = \left(\omega^2 - \frac{\Omega^2}{4}\right) \sum_{n,\,m=o}^{N} \lambda_n \lambda_m^* \mathcal{L}_{\vec{\chi}\vec{\chi}'} \left\{ d(\vec{\chi})d(\chi') \Psi_{\underline{\zeta}}(\underline{\nu}) \Psi_{\underline{\ell}_{nm}}(\underline{\nu}_{nm}) \right\} \qquad (B10)$$

The characteristic functions, $\Psi_{\underline{\zeta}}$ and $\Psi_{\underline{\ell}_{nm}}$, are determined simply from Equation (B8) and the definitions of $\underline{\nu}$, $K_{\underline{\zeta}}$, $\underline{\nu}_{nm}$, and $K_{\underline{\ell}_{nm}}$, once $\underline{\zeta}$ and $\underline{\ell}_{nm}$ are defined.

If we define the two-dimensional vector of surface roughness parameters to be

$$\underline{\zeta}^t = [\zeta, \zeta']$$

from Equation (B7), we recognize

$$\underline{\nu}^t = \left[\left(\omega - \frac{\Omega}{2}\right)\eta, \ -\left(\omega + \frac{\Omega}{2}\right)\eta \right]$$

From the assumed properties of ζ in Equation (B5)

$$K_{\underline{\zeta}} = \sigma_\zeta^2 \begin{bmatrix} 1 & \rho\zeta \\ \rho\zeta & 1 \end{bmatrix}, \quad \bar{\underline{\zeta}} = 0$$

hence

52

$$\Psi_{\underline{\zeta}}(\underline{\upsilon}) = e^{-\eta^2 \sigma_\zeta^2 \left[\left(\omega^2 + \frac{\Omega^2}{4} \right) - \left(\omega^2 - \frac{\Omega^2}{4} \right) \rho_\zeta (u, v) \right]} \tag{B11}$$

In computing $\Psi_{\underline{\ell}_{nm}}$, consider the case, $n > m$, and define the $(n + m)$ dimensional vector, $\underline{\ell}_{nm}$, to be

$$\underline{\ell}_{nm}{}^t = [\ell_1, \ell_1', \ell_2, \ell_2', \ldots, \ell_m, \ell_m', \ell_{m+1}, \ell_{m+2}, \ldots, \ell_n]$$

Then, from Equation (B7),

$$\underline{\upsilon}_{nm}{}^t = \left[\underline{\upsilon}_1, \underline{\upsilon}_2, \ldots, \underline{\upsilon}_m, \left(\omega - \frac{\Omega}{2} \right) \beta_{m+1}, \left(\omega - \frac{\Omega}{2} \right) \beta_{m+2}, \ldots, \left(\omega - \frac{\Omega}{2} \right) \beta_n \right]$$

where

$$\underline{\upsilon}_q{}^t = \left[\left(\omega - \frac{\Omega}{2} \right) \beta_q, - \left(\omega + \frac{\Omega}{2} \right) \beta_q^* \right], \quad q = 1, \cdots m$$

From the properties ascribed the ℓ_q in Equation (B6), the correlation matrix, $K_{\ell_{nm}}$, has the form

$$K_{\ell_{nm}} = \begin{bmatrix} \underset{\sim}{K}_{11} & \underset{\sim}{K}_{12} \cdots \underset{\sim}{K}_{1m} & \vdots & \\ \underset{\sim}{K}_{21} & \underset{\sim}{K}_{22} \cdots \underset{\sim}{K}_{2m} & \vdots & 0 \\ \vdots & \vdots \qquad \vdots & \vdots & \\ \underset{\sim}{K}_{m1} & \underset{\sim}{K}_{m2} \cdots \underset{\sim}{K}_{nm} & \vdots & \\ \hline & 0 & \vdots & \underset{\sim}{K}_{(n-m)} \end{bmatrix}$$

53

where the $\underset{\sim}{K}_{qp}$ are the (2 x 2) matrices

$$\underset{\sim}{K}_{qp} = \sigma_{qp}^{2} \begin{bmatrix} 1 & \rho_{qp} \\ \\ \rho_{qp} & 1 \end{bmatrix} = \underset{\sim}{K}_{pq}$$

and $\underset{\sim}{K}_{(n-m)}$ is the (n - m) x (n - m) matrix with elements

$$\sigma_{m+i,\,m+j}^{2}, \qquad 1 \le i, j \le n - m$$

Then, noting that

$$\underset{\sim}{\upsilon}_{q}^{t} \underset{\sim}{K}_{qp} \underset{\sim}{\upsilon}_{p} = \sigma_{qp}^{2} \left\{ \left(\omega - \frac{\Omega}{2}\right)^{2} \beta_{q} \beta_{p} - \left(\omega^{2} - \frac{\Omega^{2}}{4}\right) \left(\beta_{q}\beta_{p}^{*} + \beta_{q}\beta_{p}\right) \rho_{qp} \right.$$

$$\left. + \left(\omega + \frac{\Omega}{2}\right)^{2} \beta_{q}^{*} \beta_{p}^{*} \right\}$$

$$\Psi_{\underline{\ell}_{nm}}(\underset{\sim}{\upsilon}_{nm}) = e^{-j\left(\omega - \frac{\Omega}{2}\right) \overset{n}{\underset{q=o}{\Sigma}} \beta_{q}\bar{\ell}_{q} + j\left(\omega + \frac{\Omega}{2}\right) \overset{m}{\underset{q=o}{\Sigma}} \beta_{q}^{*} \bar{\ell}_{q}} \qquad (B12)$$

$$\cdot \; e^{-\frac{1}{2}\left(\omega - \frac{\Omega}{2}\right)^{2} \overset{n}{\underset{q,\,p=o}{\Sigma}} \beta_{q}\beta_{p}\sigma_{qp}^{2} - \frac{1}{2}\left(\omega + \frac{\Omega}{2}\right)^{2} \overset{m}{\underset{q,\,p=o}{\Sigma}} \beta_{q}^{*}\beta_{p}^{*}\sigma_{qp}^{2}}$$

$$\cdot \; e^{\left(\omega^{2} - \frac{\Omega^{2}}{4}\right) \overset{Q_{nm}}{\underset{q,\,p=o}{\Sigma}} \sigma_{qp}^{2} \, \text{Re}\left(\beta_{q}\beta_{p}^{*}\right) \rho_{qp}} (u, v)$$

where $Q_{nm} = \min(n, m)$.

Consider next the typical spatial integral in Equation (B7) by picking out only those terms in Equations (B11) and (B12) which are functions of $\vec{\gamma}$ and $\vec{\chi}'$. The typical integral is

54

$$J_{nm} = \int\limits_{-\infty}^{\infty}\!\!\int\!\int\!\int dx\,dy\,dx'\,dy'\, e^{-\frac{1}{2}\left(\frac{x^2 + x'^2}{Dx^2} + \frac{y^2 + y'^2}{Dy^2}\right)} \tag{B13}$$

$$\cdot\, e^{\left(\omega^2 - \frac{\Omega^2}{4}\right)\left[\eta^2 \sigma_\zeta^2 \rho_\zeta(u,v) + \sum\limits_{q,p=o}^{Q_{nm}} \sigma_{qp}^2 \, Re\left(\beta_q \beta_p^*\right)\rho_{qp}(u,v)\right]}$$

Define

$$t_{nm}^2 = \eta^2 \sigma_\zeta^2 + \sum\limits_{q,p=o}^{Q_{nm}} \sigma_{qp}^2 \, Re\left(\beta_q \beta_p^*\right) \tag{B14}$$

and a composite correlation coefficient

$$\widetilde{\rho}_{nm}(u,v) = \frac{1}{t_{nm}^2}\left[\eta^2 \sigma_\zeta^2 \rho_\zeta(u,v) + \sum\limits_{q,p=o}^{Q_{nm}} \sigma_{qp}^2 \, Re\left(\beta_q \beta_p^*\right)\rho_{nm}\right] \tag{B15}$$

Then, substituting $x = x' + u$, $y = y' + v$ and performing the x' and y' integration, J_{nm} reduces to

$$J_{nm} = \pi Dx Dy \int\limits_{-\infty}^{\infty}\!\!\int du\,dv\, e^{-\frac{1}{2}\left(\frac{u^2}{Dx^2}+\frac{v^2}{Dy^2}\right) + \left(\omega^2 - \frac{\Omega^2}{4}\right)t_{nm}^2 \widetilde{\rho}_{nm}(u,v)} \tag{B16}$$

Equation (B16) cannot be integrated exactly for the usual forms of $\widetilde{\rho}_{nm}$. However, certain reasonable functions permit approximate solutions in terms of common tabulated functions. With this goal in mind, it is assumed that $\widetilde{\rho}_{nm}$ is of the form

$$\widetilde{\rho}_{nm}(u,v) = \exp\left\{-\frac{1}{2}\left[\frac{u^2}{Lx_{nm}^2} + \frac{v^2}{Ly_{nm}^2} - \frac{2a_{nm}uv}{Lx_{nm}Ly_{nm}}\right]\right\} \tag{B17}$$

where Lx_{nm} and Ly_{nm} are correlation lengths appropriate to the principal axes of $d(\vec{\chi})$ and $0 \le a_{nm} < 1$, with $a_{nm} = 0$ when the principal axes of $\widetilde{\rho}_{nm}$ coincide with those of $d(\vec{\chi})$. Expanding the exponent

55

$$e^{\left(\omega^2 - \frac{\Omega^2}{4}\right)t_{nm}^2 \, \breve{\rho}_{nm}} = \sum_{k=0}^{\infty} \frac{\left[\left(\omega^2 - \frac{\Omega^2}{4}\right)t_{nm}^2\right]^k}{k!} \, \widetilde{\rho}_{nm}^{\ k} \tag{B18}$$

J_{nm} can be written as the series

$$J_{nm} = \sum_{k=0}^{\infty} J_{nmk} \tag{B19}$$

where J_{nmk} is of the form

$$J_{nmk} = \frac{\pi Dx Dy \left[\left(\omega^2 - \frac{\Omega^2}{4}\right)t_{nm}^2\right]^k}{k!} \int_{-\infty}^{\infty} d\underline{z} \; e^{-\frac{1}{2}\underline{z}^t K_o^{-1}\underline{z}} \tag{B20}$$

with $\underline{z}^t = [u, v]$ and

$$K_{\sim o}^{-1} = \begin{bmatrix} \left(\dfrac{1}{2Dx^2} + \dfrac{k}{Lx_{nm}^2}\right) - & \dfrac{ka_{nm}}{Lx_{nm}Ly_{nm}} \\[4ex] -\dfrac{ka_{nm}}{Lx_{nm}Ly_{nm}} & \left(\dfrac{1}{2Dy^2} + \dfrac{k}{Ly_{nm}^2}\right) \end{bmatrix} \tag{B21}$$

Equation (B20) is of the form of a bivariate gaussian integral with the result that

$$J_{nmk} = \frac{2\pi^2 Dx Dy \left[\left(\omega^2 - \frac{\Omega^2}{4}\right)t_{nm}^2\right]^k}{k! \; |K_o^{-1}|^{1/2}} \tag{B22}$$

For bottom reflections far from the transmitter and receiver, it is reasonable to assume that $Dx^2/Lx_{nm}^2 \gg 1$ and $Dy^2/Ly_{nm}^2 \gg 1$. Hence,

$$|K_{\sim o}^{-1}| \simeq \begin{cases} \dfrac{1}{2DxDy}, & k = 0 \\[4ex] \dfrac{k}{Lx_{nm}Ly_{nm}}\sqrt{1 - a_{nm}^2}, & k \geq 1 \end{cases} \tag{B23}$$

56

and

$$J_{nm}(\omega, \Omega) = (2\pi DxDy)^2 + \frac{2\pi^2 DxDy Lx_{nm} Ly_{nm}}{\sqrt{1 - a_{nm}^2}} \sum_{k=1}^{\infty} \frac{\left[\left(\omega^2 - \frac{\Omega^2}{4}\right)t_{nm}^2\right]^k}{k \cdot k!}$$

$$= (2\pi DxDy)^2 + \frac{2\pi^2 DxDy Lx_{nm} Ly_{nm}}{\sqrt{1 - a_{nm}^2}} \left[\overline{E_i}\left[\left(\omega^2 - \frac{\Omega^2}{4}\right)t_{nm}^2\right] - \gamma_E \right.$$
$$\left. - \log\left[\left(\omega^2 - \frac{\Omega^2}{4}\right)t_{nm}^2\right] \right]$$

(B24)

where $\overline{E_i}(x)$ is the exponential integral defined as [21]

$$\overline{E_i}(x) = \int_{-\infty}^{x} \frac{e^t}{t} dt$$

(B25)

and γ_E is Euler's constant.

Finally, combining the nonspatial-dependent terms of Equations (B11) and (B12) with $J_{nm}(\omega, \Omega)$, the desired integral can be written in the form

$$I(\omega, \Omega) = \left(\omega^2 - \frac{\Omega^2}{4}\right) e^{-\eta^2 \sigma_\zeta^2 \left(\omega^2 + \frac{\Omega^2}{4}\right)} \sum_{n, m=o}^{N} \lambda_n \lambda_m^* J_{nm}(\omega, \Omega) e^{-j\left(\omega - \frac{\Omega}{2}\right)\mu_n + j\left(\omega - \frac{\Omega}{2}\right)\mu_m^* - \frac{1}{2}\left(\omega - \frac{\Omega}{2}\right)\varkappa_n - \frac{1}{2}\left(\omega + \frac{\Omega}{2}\right)\varkappa_m^*}$$

(B26)

where

$$\mu_n = \sum_{q=o}^{n} \beta_q \overline{\ell_q}$$

(B27

$$\varkappa_n = \sum_{q=o}^{n} \sum_{p=o}^{n} \beta_q \beta_p \sigma_{qo}^2$$

REFERENCES

1. Stradling, C. S., "Active Sonar Target Classification: Basic Approaches to Problem Solution," Vol. I, Proceedings of the Symposium on Active Sonar Classification (U), Naval Postgraduate School, Monterey, California, October 1956.

2. Cox, H. and F. Wiekhost, "Introduction to STARLITE," Vol. II, Proceedings of the Symposium on Active Sonar Classification (U), Naval Postgraduate School, Monterey, California, October 1967.

3. Schindler, R. P., "Classification Clues in Long-Range Sonar Systems," Vol. I, Proceedings of the Symposium on Active Sonar Classification (U), Naval Postgraduate School, Monterey, California, October 1967.

4. Chernov, L. A., Wave Propagation in a Random Medium, McGraw-Hill Book Co., Inc., New York, 1960.

5. Tatarski, V. A., Wave Propagation in a Turbulent Medium, McGraw-Hill Book Co., Inc., New York, 1961.

6. Laval, R. et al., "Coherence Problems in Underwater Acoustic Propagation," SACLANT Tech. Report No. 102, NATO, 15 November 1967, (ASTIA DOC. AD826 631).

7. Tolstoy, I. and C. S. Clay, Ocean Acoustics: Theory and Experiment in Underwater Sound, McGraw-Hill Book Co., Inc., New York, 1966, Chapter 6.

8. Ol'shevskii, V. V., "Characteristics of Sea Reverberation," Consultants Bureau, New York, 1967.

9. Middleton, D., IEEE Trans. Information Theory, Vol. IT-13, Part I: 372-392, Part II: 393-414 (1967).

10. Tolstoy, I. and C. S. Clay, Op. Cit., p. 198, eq. 6.23.

11. Mackenzie, K. V., J. Acoust. Soc. Amer., Vol. 32, 221-231 (1960).

12. Nuttal, A. H. and B. F. Cron, J. Acoust. Soc. Amer., Vol. 40, 1094-1107 (1966).

13. Clay, C. S., J. Geophys. Res., Vol. 71, 2037-2046 (1966).

14. Tolstoy, I. and C. S. Clay, Op. Cit., Chapter 2, Section 5.

15. Clay, C. S. and P. A. Rona, J. Geophys. Res. Vol. 70, 855-870 (1965).

16. Menotti, F. R., S. R. Santaniello and W. R. Schumacher, J. Acoust. Soc. Amer., Vol. 38, 707-714 (1965).

17. Shumway, G., Geophysics, Vol. 25, 451-467, 659-682 (1960).

18. Wood, A. B. and D. E. Weston, Acoustica, Vol. 14, 156-162 (1964).

19. Cole, B. F., J. Acoust. Soc. Am., Vol. 38, 291-297 (1965).

20. Davenport, Jr., W. B. and W. L. Root, Random Signals and Noise, McGraw-Hill Book Co., Inc., New York, 1958, Chapter 8.

21. Jahnke, E. and F. Emde, Tables of Functions, Dover Publications, New York (1945).

22. Cook, C. E., Proc. IRE, Vol. 48, 310-316 (1960).

23. Wiekhorst, F., "STARLITE Classification Experiments Using High-Resolution FM Signals," Vol. II, Proceedings of the Symposium on Active Sonar Classification (U), Naval Postgraduate School, Monterey, California, October 1967.

CONFIDENTIAL
Security Classification

DOCUMENT CONTROL DATA - R & D

(Security classification of title, body of abstract and indexing annotation must be entered when the overall report is classified)

1. ORIGINATING ACTIVITY (Corporate author)	2a. REPORT SECURITY CLASSIFICATION
Honeywell Inc., Research Department Systems and Research Center, 2345 Walnut St. Roseville, Minnesota 55113	CONFIDENTIAL
	2b. GROUP
	4

3. REPORT TITLE

BOTTOM BOUNCE SONAR SIGNAL CHARACTERISTICS AND TARGET CLASSIFICATION (U)

4. DESCRIPTIVE NOTES (Type of report and inclusive dates)

Final Report - 12 April 1968 - 12 November 1968

5. AUTHOR(S) (First name, middle initial, last name)

Richard M. Powell
Duane H. Tack
Eugene E. Yore

6. REPORT DATE	7a. TOTAL NO. OF PAGES	7b. NO. OF REFS
January 1969	67	23

8a. CONTRACT OR GRANT NO.	9a. ORIGINATOR'S REPORT NUMBER(S)
N00024-68-C-1219	12120-FR
b. PROJECT NO.	
SF 1010316	
c.	9b. OTHER REPORT NO(S) (Any other numbers that may be assigned this report)
d. Task No. 08733	

10. DISTRIBUTION STATEMENT

11. SUPPLEMENTARY NOTES	12. SPONSORING MILITARY ACTIVITY
	Naval Ship Systems Command Washington, D. C. 20360 ATTN: Ships 00VIC

13. ABSTRACT

(C) A study of the space-time properties of active sonar echoes is made with a view toward target classification on the basis of shape and aspect at long range in the bottom bounce mode. Spectral and time cross-correlations of the echoes at two space points are examined for feasibility of signal processing with respect to requirements on the transmitted signal and transmitter-target-receiver geometries. STARLITE processing (spectral correlation) is the most promising of the two, but a detailed examination of the echo properties leads to more severe restrictions on the transmitted signal and receiver separations than previously indicated. Ideally, a wide, flat spectral window (created by the transmitted signal), within which a band-limited spectral correlation is performed, is desired. Filtering and spreading of t' e signal spectrum upon reflection off an irregular, stratified, impedance bottom distorts the spectral window. This places additional constraints upon the operational parameters for which the space-time properties of the echo yield target information beyond that which is available at a single receiver.

DD FORM **1473** REPLACES DD FORM 1473, 1 JAN 64, WHICH IS OBSOLETE FOR ARMY USE.

CONFIDENTIAL
Security Classification

14. KEY WORDS	LINK A		LINK B		LINK C	
	ROLE	WT	ROLE	WT	ROLE	WT
Acoustic impedance						
Bottom bounce echo ranging						
Classification clues						
Correlation techniques						
Reflection						
Space-time analysis						
STARLITE						